

Dear Editor,

On behalf of my co-authors, I would like to express our sincere thanks to you and the anonymous reviewers for the efforts on reviewing our manuscript entitled “Assessing the impacts of reservoirs on the downstream flood frequency by coupling the effect of the scheduling-related multivariate rainfall into an indicator of reservoir effects”(ID: hess-2019-42).

According to the reviewer's comments, the manuscript has been revised. All the comments made by the reviewers are very professional. We have carefully addressed all the comments in the revision of the manuscript. A point-by-point response to the comments and the relevant changes made in the manuscript are presented as appendix to this letter. The revised manuscript with all revisions marked in red color is appended at the end of this document.

We hope the revision of the manuscript will meet with the approval of the reviewers and editors for publication in HESS.

With all best wishes.

Yours,

Lihua Xiong

On behalf of my co-authors

State Key Laboratory of Water Resources and Hydropower Engineering Science

Wuhan University, Wuhan 430072, China

E-mail: xionglh@whu.edu.cn

Telephone: +86-13871078660

Fax: +86-27-68773568

Reply to Referee #1

This study describes a modeling framework to account for the role of reservoirs in flood frequency analysis. While I think that the topic is generally of interest to the readership of this journal, I have a number of comments that should be addressed before considering it for publication.

Response:

We are truly grateful for your positive comments and helpful suggestions. All your comments have been carefully addressed in the revised manuscript. Please see our point-by-point responses to your comments below.

-The manuscript needs to be proofread more carefully as there are several typos and unclear sentences. I will try point out some of these issues in the comments below, but this is not a complete list.

Response:

Thanks for your advice. We have carefully proofread the manuscript to correct all issues about typos and unclear expressions.

- Line 26: what “previous study”?

Response:

This has been deleted in the revised manuscript.

- Lines 46-49: which of the two references is the quote from?

Response:

This quote is summarized by Wyżga et al. (2016). In the revision, the other reference has been deleted for clarity.

- Line 49: “nature extreme flow” is unclear.

Response:

For clarity, we have changed this sentence in the revised manuscript as follows:

In general, without reservoirs, the flood extremes downstream of most rain-dominated basins are mainly related to the extreme rainfall in the drainage area...

- Line 46: “this method makes it suitable”

Response:

We can't find this sentence on Line 46. It may be on Line 75. In the revision, this sentence has been rephrased as follows:

The continuous simulation method can explicitly account for the reservoir effects on flood in the hypothetical case. However, it is difficult to apply this approach to the most real cases (Volpi et al., 2018), because the simplifying assumptions of this approach are just satisfied in a few of basins with single small reservoir. Furthermore, even if the basins meet the simplifying assumptions, the detailed information required in this approach are probably unavailable...

Newly added literature:

Volpi, E., Di Lazzaro M., Bertola M., Viglione A., and Fiori A., 2018. Reservoir Effects on Flood Peak Discharge at the Catchment Scale. Water Resources Research, 54(11): 9623-9636. <https://doi.org/10.1029/2018WR023866>

- Line 77: "the first approach". Also, please add a reference to support the statement.

Response:

Corrected. We have added the reference (please see the above response for "- Line 46, ...").

- Lines 95-96: unclear why you can't get the uncertainties in the estimates. Please clarify.

Response:

Thank you for pointing this out. We realize our statement is imprecise. This statement has been rephrased in the revised manuscript.

... Another drawback of the ML method is its inconvenience to describe the uncertainty of model parameters estimates, because the ML can only get one estimate of the model parameters through maximization of the likelihood function....

- Line 98: "all their cases"

Corrected.

- Line 104: "for the expression of the distribution"

Response:

Corrected.

- Line 106: "in the expression"

Response:

Corrected.

- Given that you use a GEV but leave the shape parameter constant (and this is fine), please add more 2-parameter distributions (e.g., lognormal, gamma, Weibull, Gumbel) which have only two parameters that you can make vary as a function of your covariates.

Response:

Thank you for this suggestion. In the revision, we have added the four 2-parameter distributions (i.e., Lognormal, Gamma, Weibull, Gumbel). The results are summarized in Table 7 (newly-added). The results indicate that for the AK and HZ station, the nonstationary Weibull distribution with the RRCI-dependent scenario has a best performance, while for the HJG station, the nonstationary Gamma distribution with the RRCI-dependent scenario is the best model. In the revision, we have added Table 1 (newly-added) to summarize the used distributions. And the Table 6 and Table 7 are deleted. Detailed analyses of all new results have been included in the revised text. In the revised manuscript, all changes to Tables and Figures are listed as follows:

< Table 1> (newly-added)

<Table 2> (Table 1 in the original manuscript; revised)

<Table 3> (Table 2 in the original manuscript; revised)

<Table 5> (Table 4 in the original manuscript; revised)

<Table 6> (Table 5 in the original manuscript; revised)

< Table 7> (newly-added)

< Table 8> (revised)

<Table 5 in the original manuscript> (deleted)

<Table 6 in the original manuscript> (deleted)

<Figure 1> (revised)

<Figure 2> (revised)

<Figure 5> (revised)

<Figure 6> (revised)

<Figure 7> (newly-added)

<Figure 8> (Figure 7 in the original manuscript; revised)

<Figure 9> (Figure 8 in the original manuscript; revised)

<Figure 9 in the original manuscript > (deleted)

- Line 132: “To analyze”

Response:

Corrected.

- Line 139: “The Eq. (1)”

Response:

Corrected.

- If I get this right, you are assuming that the sediment trapping capability of the reservoir is negligible. However, over time the amount of storage decreases. To account for the role of sediment in reducing the reservoir capacity over time, I highly recommend the use of the Brune curve to account for it. If not Brune curve, please account for it in some fashion.

Response:

Thank you for this good and insightful suggestion. To address your comment, RI is redefined to incorporate the impact of sediment on reducing the reservoir capacity over time. In the revision, RI is defined as

$$RI = \sum_{i=1}^N \left(\frac{A_i}{A_T} \right) \cdot \left(\frac{(1 - LR_i) \cdot RC_i}{\bar{Q}} \right)$$

where LR_i is the loss rate (%) of reservoir capacity in the i -th reservoir, due to the sediment deposition. RI is affected by the loss of the reservoir capacity but not too much (Figure S2), because the main reservoirs (i.e., Dangjiangkou and Ankang reservoirs) have a small loss rate no more than 15% (Table S1 and Figure S1). The estimation of LR_i has been presented in Supplementary Information.

<Table S1> (newly-added)

<Figure S1> (newly-added)

<Figure S2> (newly-added)

Equation 1 is revised.

Equation S1 is newly-added.

Equation S2 is newly-added.

- Line 157: “the greater the MRI impact”

Response:

Corrected. Note that there is a modification of the name for MRI (revised as MARI) in the revised manuscript.

- Line 158: what does “inflexible” mean in this context?

Response:

We realize that the word “inflexible” may be inappropriate. Here, what we want to express is that the reservoir scheduling will have more constraints from the MARI. For example, when MARI with a large volume occurs and its timing is near the end of flood season, the reservoir with a operation strategy of increasing flood limit water level in stages will probably face a large peak of inflow and a insufficient residual capacity due to reservoir impounding. The above explanation will be added in the revised manuscript.

- Line 161: “where”

Response:

Corrected.

- In terms of predictors, the spatial distribution of rainfall is not really captured. I can think of situations in which the same basin-averaged rainfall will have very different effects if most of the rainfall occurs far or close to the outlet. How is this addressed here?

Response:

Thank you for your comments. To capture the spatial distribution of rainfall, for the MARI event, the distance (L) between the rainfall station with the maximum rainfall and the outlet have been considered. However, the results in Figure 5 (revised) show that for HZ station with the drainage area of 142056 km², there is a weak positive linear correlation (Pearson's $r=0.24$) between L and AMDF, while for the AK station with the drainage area of 38600 km² and the HJG station 90491 km², the linear correlation between L and AMDF is not significant. In the revised manuscript, this variable is considered as candidate to capture the spatial distribution of rainfall, but this variable is not selected for the calculation of RRCI, in consideration of both the non-significance correlation with AMDF of the study stations and the very complex fitting of 5-dimension copula.

- Line 185: “marginals”

Response:

Corrected.

- Line 204: “extensively concerned” is unclear.

Response:

Revised.

- Line 208: what does “obeys nonstationary distribution” mean?

Response:

We have revised this statement as follows:

Suppose that flood variable Y_t obeys distribution $f_{Y_t}(y_t|\boldsymbol{\eta}_t)$ with the distribution parameters $\boldsymbol{\eta}_t = [\mu_t, \sigma_t, \xi]$.

- What about model selection based on the SBC index? Would you get a more parsimonious model?

Response:

Thank you for your suggestion. In the revised manuscript, we have added the SBC index. And the model selection is based on the SBC criterion. After adding four 2-parameter distributions (i.e., Lognormal, Gamma, Weibull, Gumbel), the detailed results have been summarized in Table 7 (newly-added).

- Line 254: I don't think this statement is correct, given that you would be able to say whether a more complex model should be selected over a more complex one, not if the fit is good or bad.

Response:

Thank you. This statement has been deleted. In the revised manuscript, the chi-square test has been replaced by the SBC criterion.

- Line 266: “, and was completed”

Response:

Corrected.

- Line 281: what is the definition of “timing”?

Response:

The timing is defined as the end time of MARI. In this study, the timing of MARI is equal to the occurrence time of AMDF in the year. In the revision, this definition of “timing” has been added.

- Line 303: what does “special” mean?

Response:

In the revision, this sentence has been deleted.

- Line 314: “was calculated”

Response:

Corrected.

- In fitting the copulas, the marginals were treating as stationary. Is this really the case? Please test for the presence of nonstationarities in the marginals of the predictors. If nonstationary, please account for it.

Response:

Thanks. In the revision, the change-points of the variables are tested by the Pettitt test, and then, if any, the marginal with the change-point will be addressed by the estimation method (Xiong et al., 2015). The results in Table S2 show that there are the significant change-points in the mean intensity (I) of the AK and HJG stations and in the volume (V) of the HJG station. Results in Table 5 (Table 4 in the original manuscript; revised) indicate that the consideration of the nonstationarity in these marginals makes little difference.

< Table S2> (newly-added)

- The role of the Mann-Kendall and Pettitt tests is unclear to me. First of all, the results are discussed at a very basic and superficial level. Also, if the response variable tends to change with time but because the predictors you have selected change over time as well, then whether Y is stationary or not is not very important; however, whether the relationship between predictors and predictand doesn't change over time becomes more relevant. Please fix this part.

Response:

Thanks. Here, the Mann-Kendall and Pettitt tests are indeed non-essential. We have deleted the Mann-Kendall and Pettitt tests in the revised manuscript.

It might be hard to demonstrate whether the relationship between predictors and predictand does not change over time in this study. But this issue can be covered, because under the Bayesian framework, the uncertainty of this relationship will be reflected in the posteriori distribution of model parameters.

- Lines 362-364: Please apply a correction to account for the fact you are performing multiple hypothesis testing

Response:

The correction has been made.

- Line 374: “explains”

Response:

Revised.

- Line 391: “for every certain multivariate MRI” is unclear.

Response:

Deleted.

- Line 402: “It is of interest”

Response:

Corrected.

- Line 404: “the remaining capacity of the reservoir”

Response:

Corrected.

- Line 409: “due to correspond to” is unclear

Response:

Revised.

- Line 423: “related to the construction”

Response:

Deleted.

- Line 427: “is weak”; “The comparison”

Response:

Deleted.

- Line 428: “indicates”

Response:

Corrected.

- Line 429: “in most cases”

Response:

Corrected.

- Line 435: “100-year”

Response:

Corrected.

- Line 649: “thick blue” what?

Response:

We have changed this in the revised manuscript as follows:

...the thick blue lines...

- Line 651: “The right panels are”

Response:

Corrected.

Tables (revised and newly-added)

Table 1. Summary of the probability density functions, the corresponding moments and the used link functions for nonstationary flood frequency analysis.

Distributions	Probability density functions	Moments	Link functions
Gamma (GA)	$f_Y(y \mu_i, \sigma_i) = \frac{(y)^{1/\sigma_i^2-1}}{\Gamma(1/\sigma_i^2)(\mu_i\sigma_i^2)^{1/\sigma_i^2}} \exp\left(-\frac{y}{\mu_i\sigma_i^2}\right)$ $y > 0, \mu_i > 0, \sigma_i > 0$	$E(Y) = \mu_i$ $Var(Y) = \mu_i^2 \sigma_i^2$	$g_1(\mu_i) = \ln(\mu_i)$ $g_2(\sigma_i) = \ln(\sigma_i)$
Weibull (WEI)	$f_Y(y \mu_i, \sigma_i) = \left(\frac{\sigma_i}{\mu_i}\right) \left(\frac{y}{\mu_i}\right)^{\sigma_i-1} \exp\left(-\left(\frac{y}{\mu_i}\right)^{\sigma_i}\right)$ $y > 0, \mu_i > 0, \sigma_i > 0$	$E(Y) = \mu_i \Gamma(1+1/\sigma_i)$ $Var(Y) = \mu_i^2 [\Gamma(1+2/\sigma_i) - \Gamma^2(1+1/\sigma_i)]$	$g_1(\mu_i) = \ln(\mu_i)$ $g_2(\sigma_i) = \ln(\sigma_i)$
Lognormal (LOGNO)	$f_Y(y \mu_i, \sigma_i) = \frac{1}{y\sigma_i\sqrt{2\pi}} \exp\left\{-\frac{[\log(y) - \mu_i]^2}{2\sigma_i^2}\right\}$ $y > 0, -\infty < \mu_i < \infty, \sigma_i > 0$	$E(Y) = w^{1/2} \exp(\mu_i)$ $Var(Y) = w(w-1) \exp(2\mu_i)$ $w = \exp(\sigma_i^2)$	$g_1(\mu_i) = \ln(\mu_i)$ $g_2(\sigma_i) = \ln(\sigma_i)$
Gumbel (GU)	$f_Y(y \mu_i, \sigma_i) = \frac{1}{\sigma_i} \exp\left\{\left(\frac{y-\mu_i}{\sigma_i}\right) - \exp\left(\frac{y-\mu_i}{\sigma_i}\right)\right\}$ $-\infty < y < \infty, -\infty < \mu_i < \infty, \sigma_i > 0$	$E(Y) = \mu_i - 0.57722\sigma_i$ $Var(Y) = (\pi^2/6)\sigma_i^2$	$g_1(\mu_i) = \mu_i$ $g_2(\sigma_i) = \ln(\sigma_i)$
Generalized Extreme Value (GEV)	$f_Y(y \mu_i, \sigma_i, \xi) = \frac{1}{\sigma_i} \left[1 + \xi \left(\frac{y-\mu_i}{\sigma_i}\right)\right]^{-1/\xi-1} \exp\left\{-\left[1 + \xi \left(\frac{y-\mu_i}{\sigma_i}\right)\right]^{-1/\xi}\right\}$ $y > \mu_i - \sigma_i/\xi, -\infty < \mu_i < \infty, \sigma_i > 0, -\infty < \xi < \infty$	$E(Y) = \mu_i - \frac{\sigma_i}{\xi} + \frac{\sigma_i}{\xi} \eta_i$ $Var(Y) = \sigma_i^2 (\eta_2 - \eta_1^2) / \xi^2$ $\eta_m = \Gamma(1 - m\xi)$	$g_1(\mu_i) = \mu_i$ $g_2(\sigma_i) = \ln(\sigma_i)$

Table 2. Seven nonstationary scenarios for the formulas of the two distribution parameters (i.e., μ_t and σ_t).

Scenario classification	Scenario codes	The formula of distribution parameters	
		$g_1(\mu_t)$	$g_2(\sigma_t)$
Stationary (S0)	S0	α_0	β_0
	S11	$\alpha_0 + \alpha_1 \text{RI}$	β_0
RI-dependent (S1)	S12	α_0	$\beta_0 + \beta_1 \text{RI}$
	S13	$\alpha_0 + \alpha_1 \text{RI}$	$\beta_0 + \beta_1 \text{RI}$
RRCI-dependent (S2)	S21	$\alpha_0 + \alpha_1 \text{RRCI}$	β_0
	S22	α_0	$\beta_0 + \beta_1 \text{RRCI}$
	S23	$\alpha_0 + \alpha_1 \text{RRCI}$	$\beta_0 + \beta_1 \text{RRCI}$

Table 3. Information of the five major reservoirs in Hanjiang River basin.

Reservoirs	Longitude	Latitude	Area (km ²)	Year	Capacity (10 ⁹ m ³)
Shiquan	108.05	33.04	23400	1974	0.566
Ankang	108.83	32.54	35700	1992	3.21
Huanglongtan	110.53	32.68	10688	1978	1.17
Dangjiangkou	111.51	32.54	95220	1967	34.0
Yahekou	112.49	33.38	3030	1960	1.32

Table 5. Correlation coefficients between RRCI and AMDF.

Subset of rainfall variables	AK			HJG			HZ		
	Pearson	Kendall	Spearman	Pearson	Kendall	Spearman	Pearson	Kendall	Spearman
<i>-*</i>	-0.37	-0.18	-0.28	-0.55	-0.37	-0.54	-0.53	-0.38	-0.55
<i>M</i>	-0.27	-0.27	-0.37	-0.67	-0.53	-0.74	-0.45	-0.37	-0.51
<i>I</i>	-0.26	-0.25	-0.34	-0.74	-0.57	-0.79	-0.54	-0.41	-0.56
<i>V</i>	-0.32	-0.28	-0.39	-0.63	-0.49	-0.69	-0.57	-0.48	-0.65
<i>T</i>	-0.11	-0.17	-0.24	-0.68	-0.55	-0.73	-0.48	-0.40	-0.57
<i>M, I</i>	-0.37	-0.28	-0.38	-0.70	-0.56	-0.77	-0.56	-0.43	-0.58
<i>M, V</i>	-0.42	-0.29	-0.40	-0.64	-0.50	-0.71	-0.56	-0.45	-0.60
<i>M, T</i>	-0.37	-0.26	-0.36	-0.69	-0.57	-0.77	-0.64	-0.46	-0.63
<i>I, V</i>	-0.46	-0.31	-0.42	-0.71	-0.54	-0.76	-0.65	-0.50	-0.67
<i>I, T</i>	-0.34	-0.22	-0.31	-0.73	-0.60	-0.80	-0.68	-0.50	-0.66
<i>V, T</i>	-0.43	-0.28	-0.39	-0.68	-0.55	-0.75	-0.69	-0.52	-0.71
<i>M, I, V</i>	-0.49	-0.31	-0.42	-0.65	-0.53	-0.74	-0.63	-0.47	-0.63
<i>M, I, T</i>	-0.41	-0.27	-0.37	-0.68	-0.57	-0.78	-0.67	-0.49	-0.66
<i>M, V, T</i>	-0.50	-0.29	-0.40	-0.65	-0.56	-0.76	-0.67	-0.49	-0.67
<i>I, V, T</i>	-0.51	-0.31	-0.41	-0.67	-0.58	-0.78	-0.71	-0.53	-0.70
<i>M, I, V, T</i>	-0.53	-0.31	-0.42	-0.65	-0.57	-0.77	-0.69	-0.52	-0.69

*The values in the first row are the correlation coefficients between RI and flood series.

Table 6. Results of copula models for scheduling-related rainfall variables.

Stations	Scheduling-related variables	Pairs	Copula type	Parameters θ_c	Kendall's tau	Goodness-of-fit test based on the empirical copula	
						CvM*	p-value
AK	M, I, V, T	14	Clayton	0.16	0.08	0.169	0.86
		13	Clayton	1.28	0.39		
		12	Clayton	1.01	0.33		
		24 1	Frank	1.21	0.17		
		23 1	Frank	-2.24	-0.24		
		34 12	Clayton	0.96	0.11		
HJG	I, T	24	Clayton	1.37	0.41	0.473	0.425
HZ	I, V, T	24	Gumbel	1.12	0.11	0.181	0.82
		23	Clayton	1.31	0.40		
		34 2	Clayton	0.49	0.20		

* CvM is the statistic of the Cramer-von Mises test; if the p-value of the C-vine copula model is less than the significance level of 0.05,

the model is considered to be not consistent with the empirical copula.

Table 7. Summary of results of the nonstationary flood distribution models.

Stations	Covariates	Distributions	Selected models	The optimal formulas* of distribution parameters			AIC	SBC
				μ_t	σ_t	ξ		
AK	RI	GA	WEI_S23	exp(9.24-2.64RI)	exp(-0.769+2.9RI)	-	1177.2	1185.5
	RI	WEI		exp(9.36-2.83RI)	exp(0.882-3.18RI)	-	1176.9	1185.3
	RI	LOGNO		exp(9.14-3.86RI)	exp(-0.716+3.28RI)	-	1180.4	1188.8
	RI	GU		11875-13093RI	exp(8.5)	-	1199.6	1205.9
	RI	GEV		7685-15252RI	exp(8.3)	-0.043	1182.3	1190.6
	RRCI	GA		exp(9.28-1.11RRCI)	exp(-0.825+0.689RRCI)	-	1165.3	1173.7
	RRCI	WEI		exp(9.4-1.17RRCI)	exp(0.982-0.884RRCI)	-	1163.8	1172.2
	RRCI	LOGNO		exp(9.19-1.33RRCI)	exp(-0.749+0.677RRCI)	-	1168.0	1176.4
	RRCI	GU		12555-7535RRCI	exp(8.4)	-	1188.0	1194.2
	RRCI	GEV		8460-6722RRCI	exp(8.2)	-0.096	1172.1	1180.5
HJG	RI	GA	GA_S21	exp(9.7-1.62RI)	exp(-0.25)	-	1139.9	1146.0
	RI	WEI		exp(9.75-1.56RI)	exp(0.27)	-	1141.4	1147.5
	RI	LOGNO		exp(9.47-1.8RI)	exp(-0.17)	-	1140.9	1147.1
	RI	GU		17955-14399RI	exp(8.8)	-	1189.5	1195.7
	RI	GEV		6976-5930RI	exp(8.79-1.49RI)	0.43	1149.9	1160.2
	RRCI	GA		exp(9.99-1.99RRCI)	exp(-0.45)	-	1112.5	1118.6
	RRCI	WEI		exp(10.1-1.97RRCI)	exp(0.53)	-	1113.2	1119.4
	RRCI	LOGNO		exp(9.75-1.94RRCI)	exp(-0.38)	-	1113.9	1120.1
	RRCI	GU		23067-20871RRCI	exp(9.2-1.7RRCI)	-	1121.3	1129.6
	RRCI	GEV		12113-10683RRCI	exp(9.2-2.01RRCI)	0.051	1112.5	1122.8
HZ	RI	GA	WEI_S21	exp(9.85-2.87RI)	exp(-0.42)	-	1198.3	1204.9
	RI	WEI		exp(9.94-2.79RI)	exp(0.49)	-	1198.6	1204.9
	RI	LOGNO		exp(9.63-2.93RI)	exp(-0.33)	-	1201.1	1207.4
	RI	GU		18661-23706RI	exp(8.8)	-	1237.5	1243.7
	RI	GEV		9605-13545RI	exp(9.03-2.56RI)	0.099	1207.8	1218.3
	RRCI	GA		exp(9.85-1.52RRCI)	exp(-0.61)	-	1173.1	1179.4
	RRCI	WEI		exp(9.92-1.42RRCI)	exp(0.73)	-	1171.2	1177.5
	RRCI	LOGNO		exp(9.72-1.55RRCI)	exp(-0.51)	-	1178.7	1185.0
	RRCI	GU		19214-14344RRCI	exp(8.86-0.881RRCI)	-	1189.7	1198.1
	RRCI	GEV		12502-9911RRCI	exp(8.96-1.37RRCI)	-0.068	1176.0	1186.4

*The model parameters in the optimal formulas are the posterior mean from Bayesian inference.

Table 8. Summary of the rainfall information for the five largest floods after the construction (1967) of Danjiangkou reservoir in HZ station.

Year	Values (Ranking in 1967-2015)				
	AMDF [m ³ /s]	OR_JEP [-]	<i>I</i> [mm]	<i>V</i> [mm]	<i>T</i> [day of the year]
1983	25600 (1)	0.435 (2)	20.2 (1)	121.4 (19)	281 (2)
1975	19900 (2)	0.557 (7)	9.6 (18)	163.6 (13)	277 (6)
1974	18200 (3)	0.506 (4)	12.0 (7)	120.4 (20)	278 (4)
2005	16800 (4)	0.651 (11)	8.2 (27)	179.7 (10)	278 (4)
1984	16100 (5)	0.461 (3)	9.9 (15)	256.3 (4)	273 (9)

Figures (revised and newly-added)

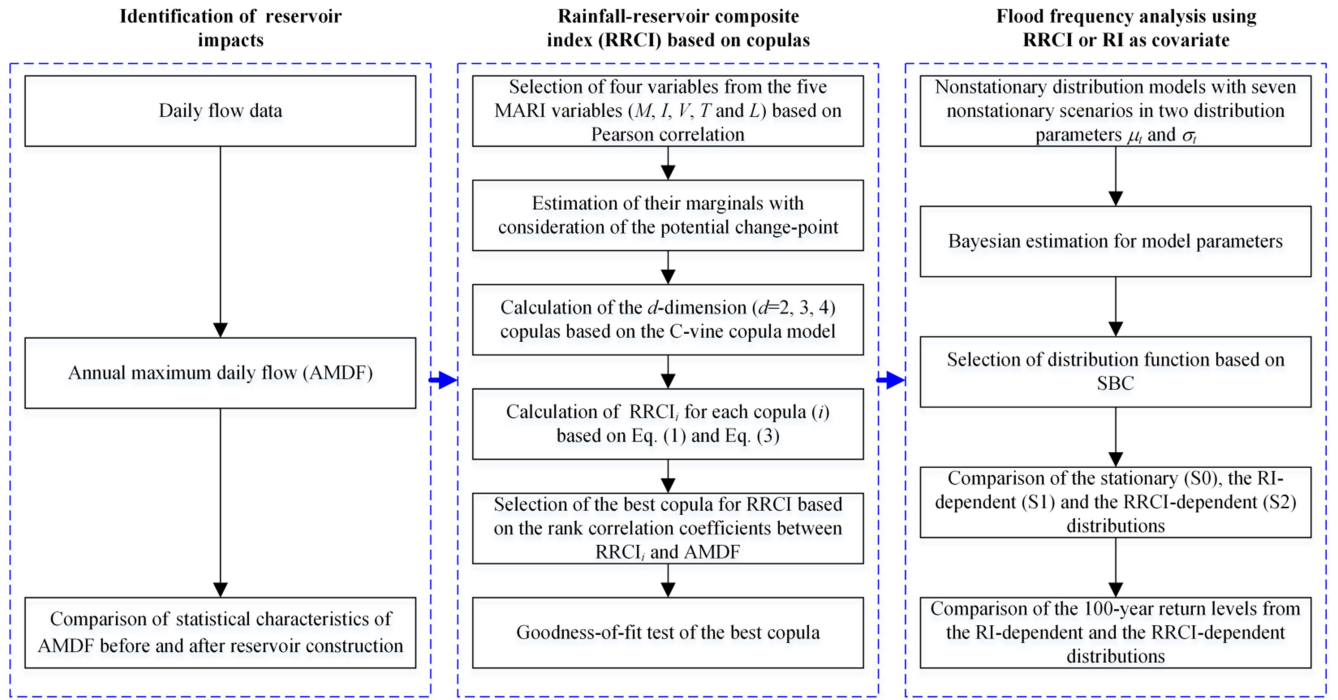


Figure 1. Flowchart of nonstationary covariate-based flood frequency analysis

with a rainfall-reservoir composite index (RRCI).

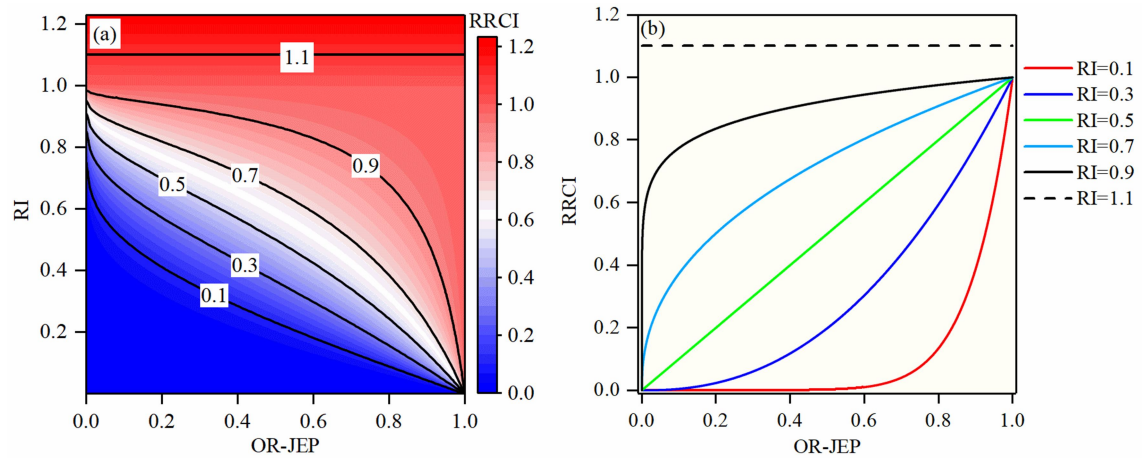


Figure 2. Relationship in the Eq. (2). (a) is the contour plot of RRCI against both RI and OR-JEP; (b) is the function curves of RRCI against OR-JEP under the different values of RI.

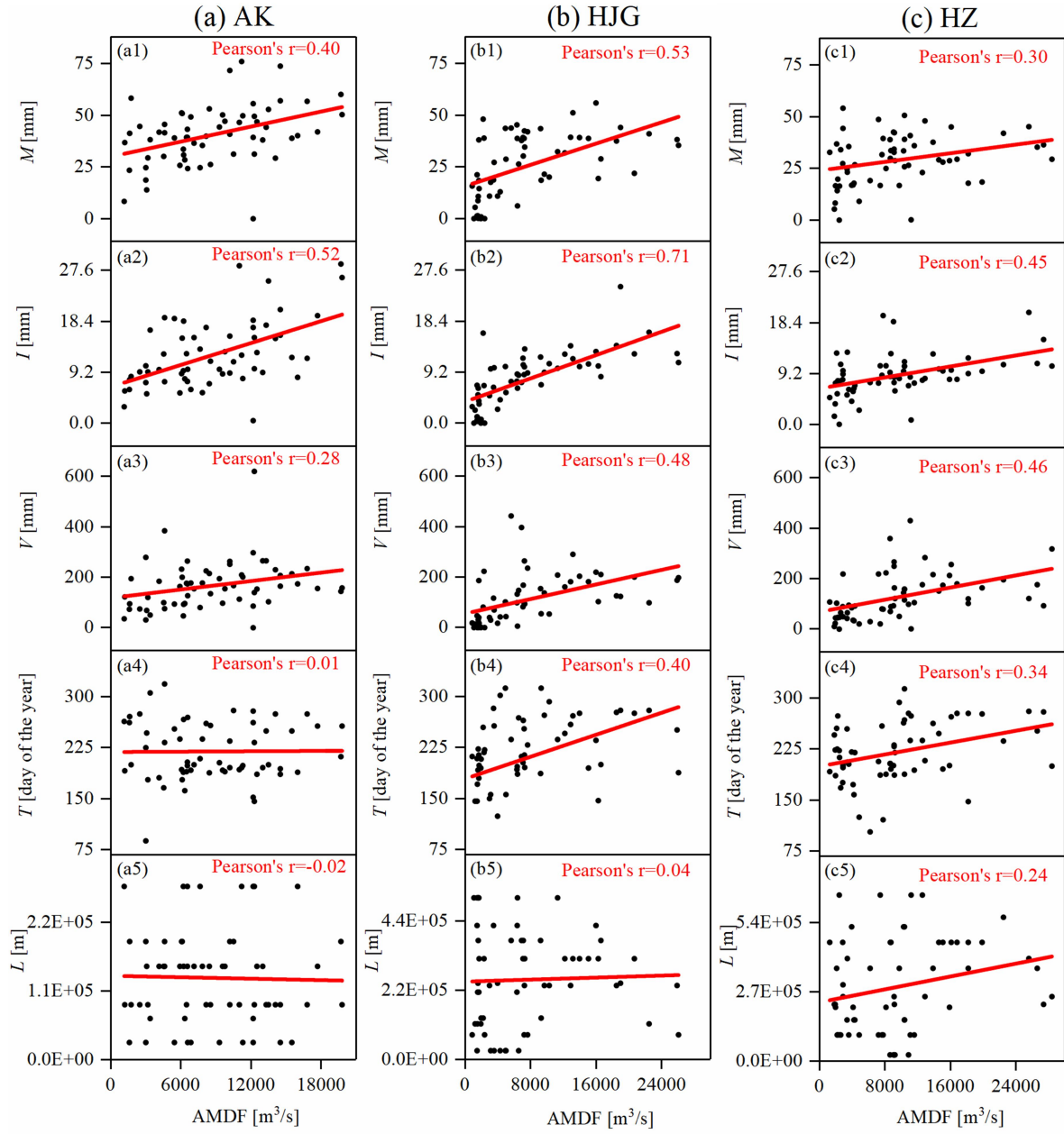


Figure 5. Linear correlation between the five MARI variables and AMDF for

(a) AK station, (b) HJG station and (c) HZ station.

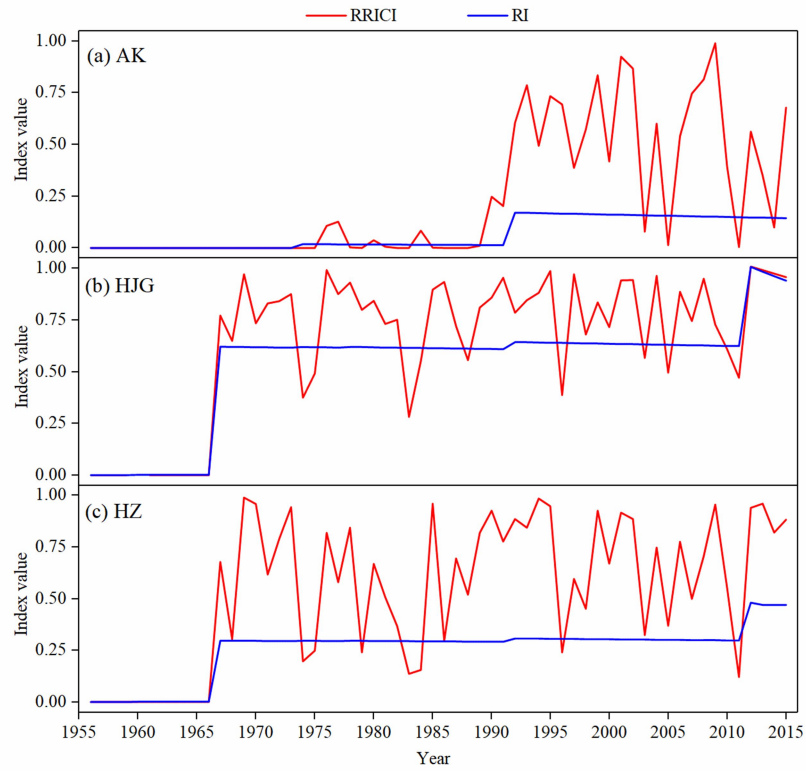


Figure 6. Variation of RI and RRICI for (a) AK station, (b) HJG station and (c)

HZ station.

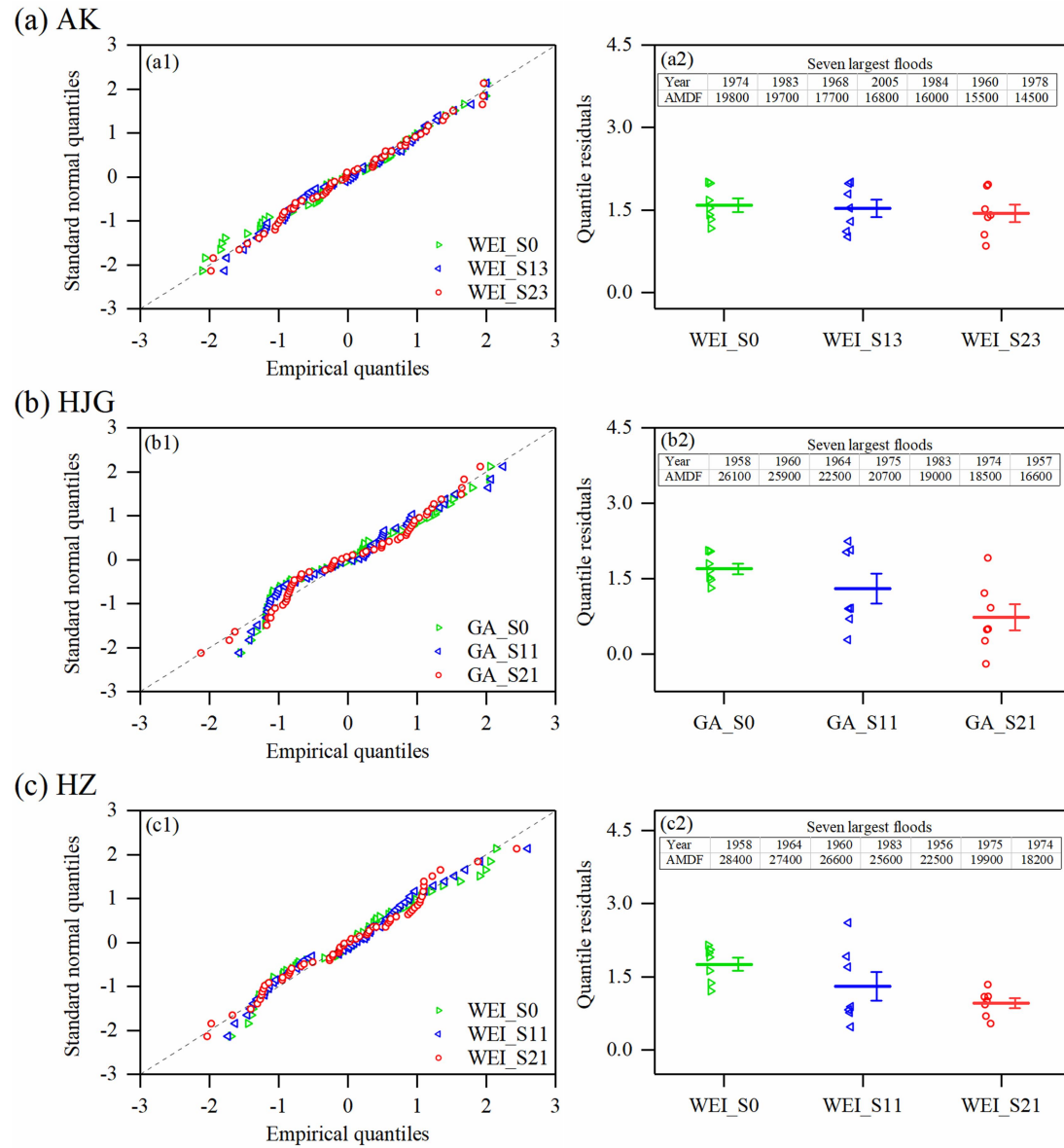


Figure 7 Comparison of the stationary (S0), the RI-dependent (S1) and the RRCI-dependent (S2) scenarios of the same optimal distributions for (a) AK station, (b) HJG station and (c) HZ station. The left panels (a1, b1 and c1) are the QQ plots for the whole AMDF series in each station. The right panels (a2, b2 and c2) are the plots of quantile residuals for the seven largest floods (their values and occurrence years have been listed) in each station, and the means of their quantile residuals (points) and the corresponding standard errors are indicated by the lines.

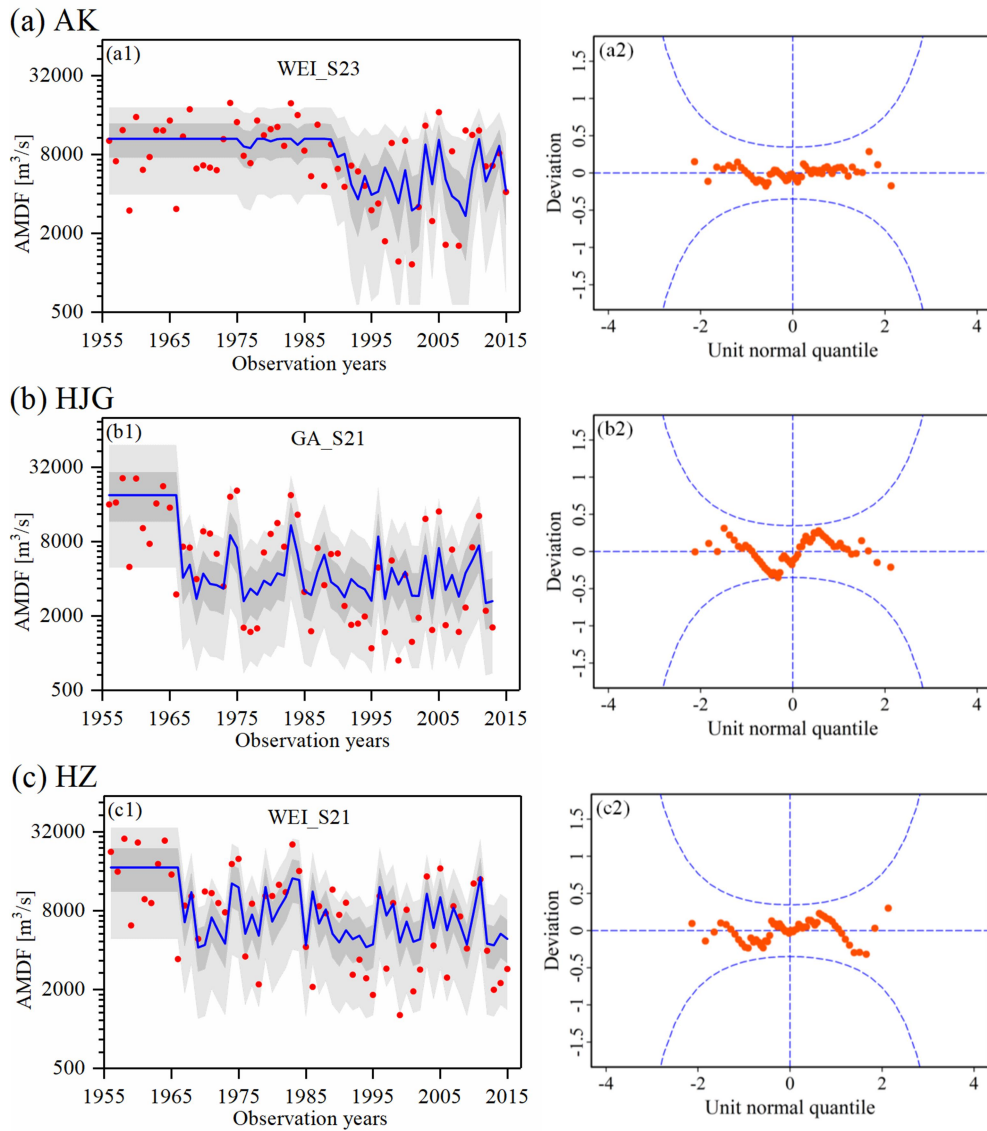


Figure 8. Performance of (a) WEI_S23 for AK station, (b) GA_S21 for HJG station and (c) WEI_S21 for HZ station. The left panels (a1, b1 and c1) are the centile curves plots in each station (the 50th centile curves are indicated by the thick blue lines; the light gray-filled areas are between the 5th and 95th centile curves; the dark grey-filled areas are between the 25th and 75th centile curves; the filled red points indicate the observed series). The right panels (a2, b2 and c2) are the worm plots; a reasonable model should have the plotted points within the 95% confidence intervals (between the two blue dashed curves).

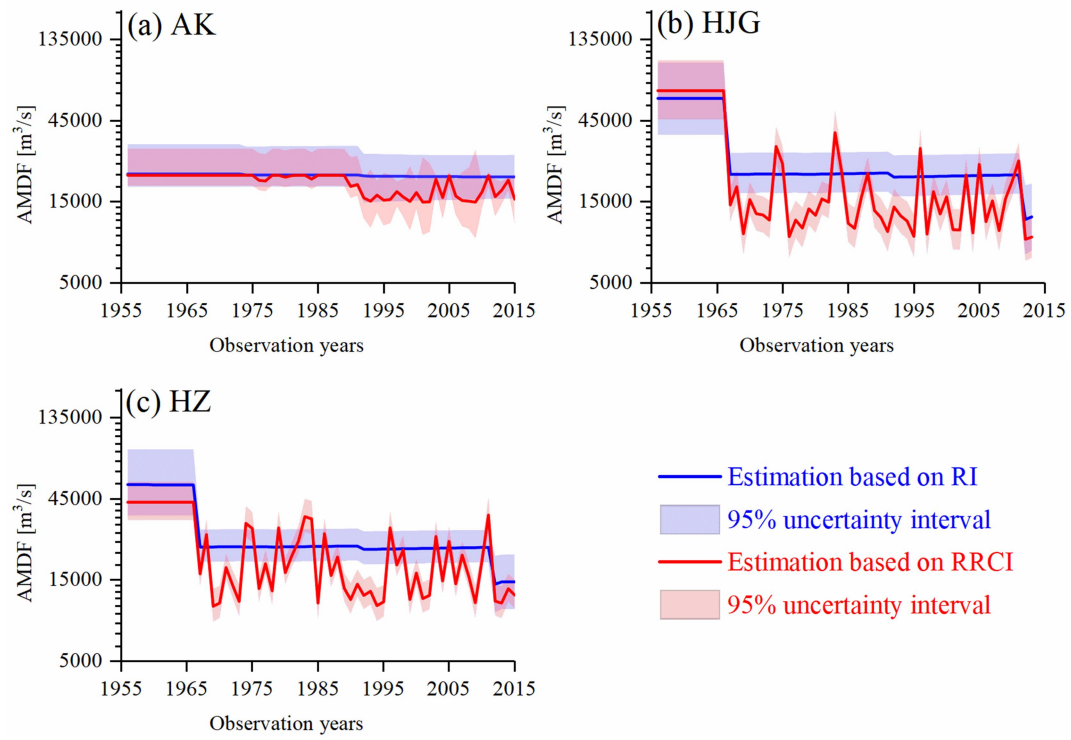


Figure 9. Statistical inference of the 100-year return levels with the 95% uncertainty interval using the optimal RI-dependent and RRCI-dependent distributions: (a) WEI_S13 and WEI_S23 for AK station, (b) GA_11 and GA_S21 for HJG station, and (c) WEI_S11 and WEI_S21 for HZ station.

Supplementary Information

Estimation of the loss rate (%) of reservoir capacity

To estimate the variation of LR_i over time, it is assumed that there is the same amount of sediment in each year. Then, LR_i is estimated by

$$LR_i = \frac{n_i \cdot L_i^m}{RC_i} = \frac{n_i \cdot w_i^s \cdot Te_i}{\rho \cdot RC_i} \quad (S1)$$

where n_i is the number of years which the i -th reservoir has been used, L_i^m is the mean of annual loss of reservoir capacity (m^3) for the i -th reservoir, w_i^s is the mean of annual inflow sediment mass (kg) for the i -th reservoir, ρ is the density of the deposited sediment (kg/m^3) and Te_i is the trap efficiency (%). Based on the Brune method (Brune, 1953; Mulu and Dwarakish, 2015), the trap efficiency is estimated with reservoir capacity-inflow ratio as follows

$$Te_i = 1 - \frac{0.5}{\sqrt{RC_i / I_i^m}} \quad (S2)$$

where I_i^m is the mean of annual inflow volume in the i -th reservoir (m^3/day). The data in the previous literature (Guo, 1995; Hu, 2009; Liu, 2017) are collected to control the estimation errors of L_i^m . Please see Table S1.

Reference:

- Hu, A.Y., 2009. Analysis of sedimentation characteristics of Danjiangkou Reservoir. Research in Soil and Water Conservation, 16(5):237-240. (In Chinese)
- Brune, G.M., 1953. Trap Efficiency of Reservoirs. Trans. Am. Geophysical Union, 34 (3), 407-418.
- Guo, J.M., 1995. Analysis of sedimentation in Ankang Reservoir and its impact on the reservoir operation. Northwest Hydropower, 1995(3):9-12. (In Chinese)
- Liu, J.X., 2017. Sedimentation characteristic analysis and desilting scheme optimization of Shiquan Reservoir. Pearl River, 38(1): 56-59. (In Chinese)
- Mulu, A., and Dwarakish G. S., 2015. Different Approach for Using Trap Efficiency for Estimation of Reservoir Sedimentation. An Overview, Aquatic Procedia, 4, 847-852.

Table S1. Summary for the calculation of the mean of annual loss of reservoir

capacity

Reservoirs	RC_i (10^9 m^3)	I_i^m (10^9 m^3)	w_i^s (10^9 kg)	Tc_i (%)	L_i^m (10^9 m^3)	
					From previous studies	From Eq.(S2)*
Shiquan	0.566	11.73	12.6	88%	0.006	0.008
Ankang	3.21	19.17	27.1	94%	-	0.018
Huanglongtan	1.17	6.12	8.58	94%	0.007	0.006
Dangjiangkou	34.0	39.48	59.8	97%	0.044	0.042
Yahekou	1.32	1.09	-	98%	0.007	-

* $\rho = 1400 \text{ kg/m}^3$

Table S2. Results of the change-point detection for the four MARI variables.

Variables	AK		HJG		HZ	
	change-point	p-value*	change-point	p-value	change-point	p-value
<i>M</i>	1976	1.037	1989	0.371	1971	1.278
<i>I</i>	1987	0.031	1985	0.009	1990	0.080
<i>V</i>	2009	0.746	1984	0.042	1984	0.769
<i>T</i>	1992	1.180	1984	0.986	1984	1.367

*Less than 0.05 is considered significant.

Figure S1. Interannual variation of loss rate of reservoir capacity for each reservoir in the study area.

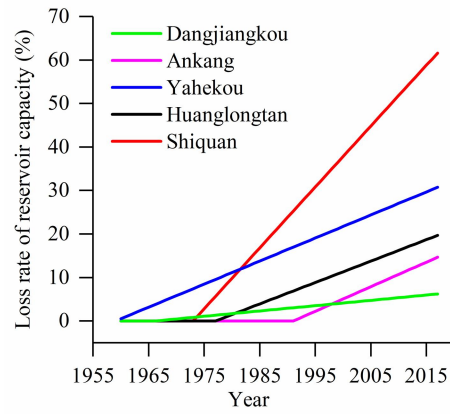


Figure S2. Impact of reservoir capacity loss on RI for AK, HJG and HZ

stations.

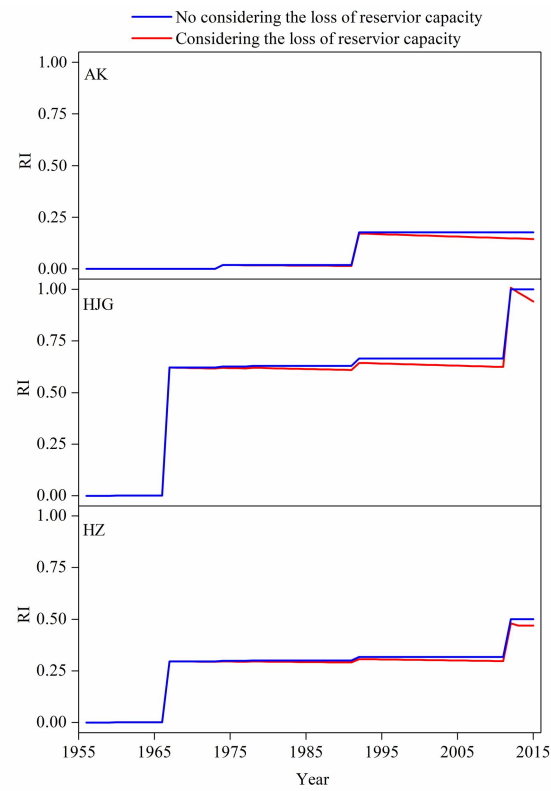
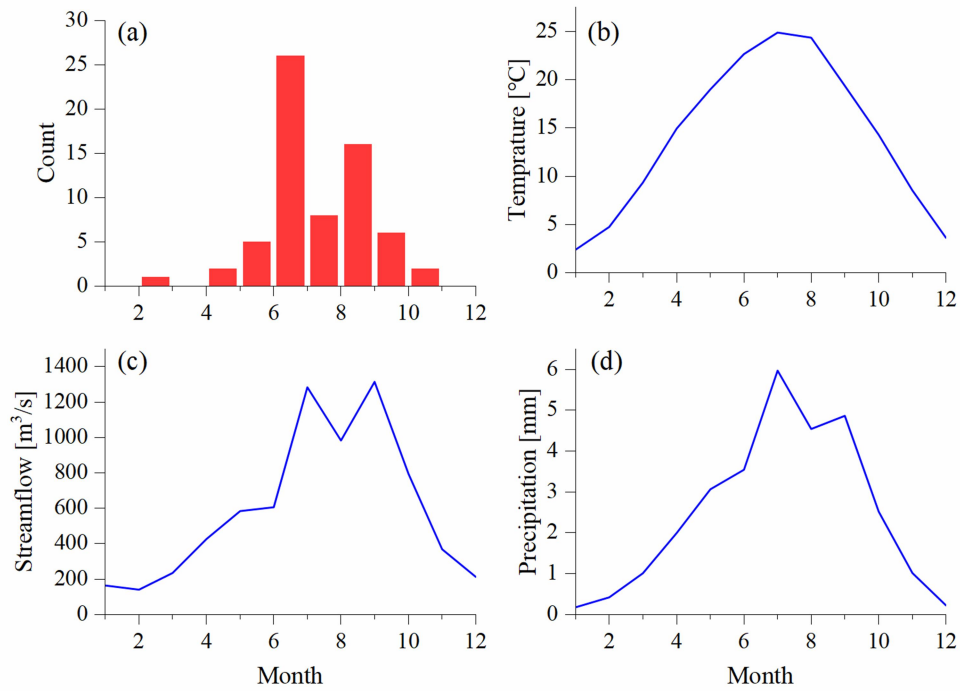


Figure S3. Preliminary analysis of the snowmelt influences on the streamflow in the catchment upstream the AK station. (a) is the total number of times for AMDF in each month; (b) is the monthly average temperature; (c) is the monthly average streamflow; and (d) is the monthly average precipitation.



Glossary and Notation:

$\alpha_0, \alpha_1, \beta_0, \beta_1$: parameters of nonstationary model.

A_i : total basin area upstream of the i -th reservoir.

A_T : total basin area upstream of the gauge station.

AIC: Akaike information criterion.

AK: Ankang (gauging station).

AMDF: annual maximum daily flow (series).

CDF: Cumulative distribution function

d : dimension of copulas.

df : freedom degree.

GA: Gamma distribution

GEV: Generalized Extreme Value distribution.

GEV_S23: nonstationary GEV distribution with the S23 scenario.

GML: generalized maximum likelihood (method).

GU: Gumbel distribution.

HJG: Huangjiagang (gauging station).

HZ: Huang zhuang (gauging station).

I : intensity, the mean of daily rainfall in MARI.

IDW: Inverse distance weighting method.

IRI: impounded runoff index, a ratio of reservoir capacity to mean annual runoff.

\hat{l} : maximized likelihood of the model object.

L : distance, the distance between the rainfall center and the outlet.

LOGNO: Lognormal distribution.

LR_i : loss rate (%) of total storage capacity of the i -th reservoir due to the sediment deposition.

μ_t : mu parameter of the distribution functions used.

M_c : length of the Markov chain.

M : maximum, the maximum of daily rainfall in MARI.

MARI: multiday antecedent rainfall input.

MCMC: Markov chain Monte Carlo.

ML: maximum likelihood (method).

n : number of data points.

N : total number of reservoirs upstream of the gauge station.

OR-JEP: OR-joint exceedance probability.

P_{MARI}^{\vee} : OR-joint exceedance probability.

θ_i : parameter vector of the i -th marginal distribution.

θ_c : copula parameter vector.

θ : parameter vector of the whole n -dimensional distribution.

$\theta_{\text{GEV_S23}}$: parameters of the GEV_S23 model.

$\hat{\theta}_{\text{GEV_S23}}^i$: an estimation for the parameters of the GEV_S23 model.

\bar{Q} : mean annual runoff.

RRCI: rainfall-reservoir composite index.

RI: reservoir index.

RC: reservoir capacity.

RC_i : total storage capacity of the i -th reservoir.

σ_i : sigma parameter of the distribution functions used.

S0: constant scenario.

S1: RI-dependent scenarios.

S2: RRCI-dependent scenarios.

SBC: Schwarz Bayesian criterion.

T : timing, the end time of MARI in the year.

u_i : univariate marginal distribution of X_i .

V : volume, the total of daily rainfall in MARI.

WEI: Weibull distribution.

ξ : shape parameter of the Generalized Extreme Value distribution.

X_1, X_2, \dots, X_d : scheduling-related MARI variables.

Reply to Referee #2

General Comments:

The manuscript presents downstream flood frequency analysis framework using the annual maximum daily flows (AMDF). Joint cumulative probability of multiple rainfall variables (maximum, intensity, volume and timing) are considered as multiday rainfall input (MRI) and employed in C-vine copula model. Flood frequency model is defined by nonstationary generalized extreme value (NGEV) distribution model including uncertainty deliberation with Bayesian approach. Rainfall reservoir composite index (RRCI) is proposed and used to quantify the reservoir effects as covariate for expression of distribution parameters. According to the different metrics, the results of the proposed method outperforms typical reservoir index (RI) based flood frequency model which only accounts reservoir capacity and mean annual runoff. I believe the study is quite interesting for the readership of the journal and contributing to better modeling of downstream flood peak mechanism. The model results give reasonable outcomes and can be useful for regions where large reservoirs are located. The manuscript deserves publication after a major revision considering my below comments.

Response:

Thank you very much for the good summary and the positive evaluation of the paper. All your valuable comments have been carefully addressed in the revision. Please see our point to point replay below.

- Language needs some refinements before publication. Also, there are some typos and repeated sentences, which make hard to follow and disturb the readability. It would be nice to revise the manuscript totally by dividing long sentences and eliminating the repeated ones. Same tense should be used (is or was) thought the text.

Response:

Thanks for your kind suggestion. We have carefully revised the text to correct all issues about typos, unclear long sentences, repeated sentences and different tenses.

- Studies dealing with downstream hydrograph alterations caused by dams are not discussed enough in the literature.

Response:

In the first paragraph of the modified version, we have added literature review on studies dealing with downstream hydrograph alterations caused by dams as follows:

....In the literature, the significant hydrological alterations caused by reservoirs are demonstrated in the many areas of the world. Graf (1999) showed that the dams have greater effects on the streamflow than the global climate change in America. Benito and Thorndycraft (2005) reported various significant changes of the

pre- and post-dam hydrologic regimes (e.g., minimum and maximum flows over different durations) across the United States. Batalla et al. (2004) demonstrated an evident reservoir-induced hydrologic alteration in the North-Eastern Spain. Yang et al. (2008) indicated the spatial variability of the hydrological regimes alteration caused by the reservoirs in the middle and lower Yellow River, China. Mei et al. (2015) found that the Three Gorges Dam, the largest dam in the world, has significantly changed the downstream hydrological regimes. In recent years, the cause-effect mechanisms of the downstream flood peak reduction were also investigated in some literature (Ayalew et al., 2013; 2015; Volpi et al., 2018). For example, Volpi et al. (2018) suggested that for a single reservoir, the downstream flood peak reduction is mainly dependent on its position along the river, its spillway and its storage capacity based on a parsimonious instantaneous unit hydrograph-based model. These studies have revealed that it is crucial to assess the impacts of reservoirs on downstream flood regimes for the success of downstream flood risk management.

Newly added literature

Ayalew, T.B., Krajewski W.F., Mantilla R., 2015. Insights into Expected Changes in Regulated Flood Frequencies due to the Spatial Configuration of Flood Retention Ponds. *Journal of Hydrologic Engineering*, 20(10): 04015010.

Graf, W.L., 1999. Dam nation: A geographic census of American dams and their large - scale hydrologic impacts. *Water resources research*, 35(4): 1305-1311.

Mei, X., Dai, Z., Van Gelder, P.H.A.J.M., and Gao, J., 2015. Linking Three Gorges Dam and downstream hydrological regimes along the Yangtze River, China. *Earth and Space Science*, 2(4): 94-106.

Volpi, E., Di Lazzaro M., Bertola M., Viglione A., and Fiori A., 2018. Reservoir Effects on Flood Peak Discharge at the Catchment Scale. *Water Resources Research*, 54(11): 9623-9636.

Yang, T., Zhang Q., Chen Y.D., Tao X., Xu C.Y., and Chen X., 2008. A spatial assessment of hydrologic alteration caused by dam construction in the middle and lower Yellow River, China. *Hydrological Processes: An International Journal*, 22(18): 3829-3843.

- As stated in Lines 45-49, there are several factors for the generation of the floods. Authors focused on meteorological conditions, but also indicating the importance of hydrological conditions such as snow cover. The elevation range of the study area is quite wide (13 – 3493 m) and most upstream reservoirs (especially Ankang gauge) should be dominated by snowmelt. The response of the basin will be complex compared to lower altitude basins. There is not much information about the assessment of the snowmelt contribution of the catchments and their effects on operational decisions. It is also interesting to see that linear correlations between the timing variable of multivariate MRI and AMDF give lowest (almost zero) Pearson r for AK gauge in Figure 5. Would snowmelt be a reason for this? If this is the case, maybe RRCI is not enough to explain downstream peak floods for the regions where

reservoirs fed by snowmelt? Temperature data can also be effective to estimate flood peaks in such cases. I believe this situation should be clarified.

Response:

Thank you for this comment. Although the elevation range of the study area is quite wide (13–3493 m), the study area is a rainfall-dominated area and the snowmelt contribution is quite limited. This area has a warm temperate semi-humid continental monsoon climate. The temperature in the basin is not much different from upstream to downstream. The timing of flood is the main rainfall period from June to September (Figure S3a, c and d). And the winter is warm as shown in Figure S3b. It is indicated that the rainfall is the main contribution for floods. The above information will be added in the revised manuscript.

<Figure S3> (newly-added)

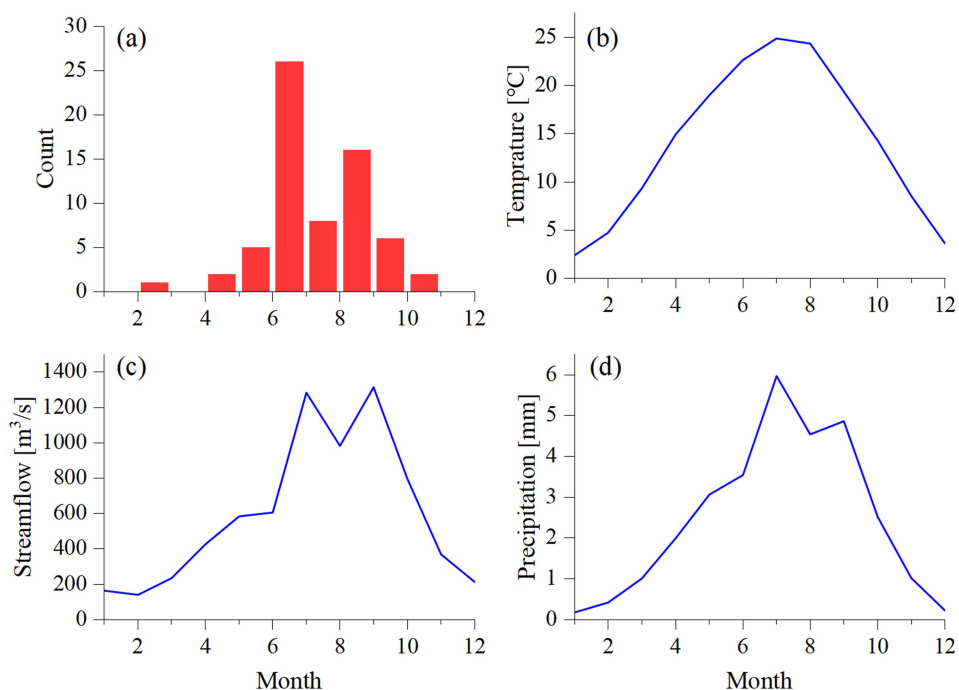


Figure S3. Preliminary analysis of the snowmelt influences on the streamflow in the catchment upstream the AK station. (a) is the total number of times for AMDF in each month; (b) is the monthly average temperature; (c) is the monthly average streamflow; and (d) is the monthly average precipitation.

The reason why AK gauge has a weak linear correlation between the timing variable of multivariate MRI and the annual maximum flood in Figure 5 is probably that there is a non-significant effect of the staged operation of the reservoirs on the floods. The reservoirs upstream of AK station have a smaller capacity than HJG and HZ stations. There may be a random variation of the remaining storage capacity in each staged period of the flood season for AK station. Thus, in the long term, the reduction of the peaks of AK station tends to be not different in each staged period of the flood season.

And Figure S3 has been added in Supplementary Information.

- In Data Section, the explanation of reservoir data is based on only their capacities. There is not much information how they are operated. For example, for what purposes they are operated, or how their reservoir pools are divided (flood control, conservation, dead storage etc.)?

Response:

Agree. In the revision, more information on the reservoir operation has been added as follows:

... The Danjiangkou Reservoir in central China's Hubei province is the largest one in this basin, and was completed by 1967. As a multi-purpose reservoir, it mainly aims to supply water and control floods, and is also used for electricity generation and irrigation. The reservoir has the total storage capacity of 21.0 billion m³, the dead storage capacity of 7.23 billion m³, the effective storage capacity of 10.2 billion m³, and the flood control capacity of 7.72 billion m³. After the Danjiangkou Dam Extension Project in 2010, the Danjiangkou Reservoir gained an additional capacity of 13.0 billion m³ and an extra flood control storage capacity of 3.3 billion m³. Besides, this reservoir is operated by the strategy of staged increasing flood limit water level in the flood control season (Zhang et al., 2009).

Newly added literature

Zhang L., Xu J., Huo, J., Chen J., 2009. Study on Stage Flood Control Water Level of Danjiangkou Reservoir. Journal of Yangtze River Scientific Research Institute, 26 (3): 13-14. (In Chinese)

- It is not clear why inverse distance weighting (IDW) is selected for areal distribution of the rainfall records. The catchments are large and elevation ranges in between 13-3493 m, so that this method may not be representative especially for mountainous regions.

Response:

The reason why IDW is selected is that IDW is a handy method. Due to both the data limitation (16 sites) and the unstable relationship between rainfall and elevation, it is hard for us to demonstrate whether the other methods (e.g., the Kriging methods) will be better. In this study, the rainfall records from all national meteorological stations in the study area are used. The precision of areal rainfall with the IDW method should be able to meet the requirement in the study. In the revision, the error of estimation of areal rainfall has been discussed to remind readers in the discussion as follows:

...The areal-averaged MARI is based on the records of 16 rainfall stations with the IDW method; the estimation error of areal-averaged rainfall may be transferred to the OR-JEP estimation error; the additional rainfall site data and spatial distribution information are needed to reduce the OR-JEP estimation error. Nonetheless, the good performance of downstream flood frequency modeling demonstrates the MARI samples still remain representative in this study.

- Maybe it would be better to call “downstream flood frequency analysis” rather than “flood frequency analysis” throughout the manuscript?

Response:

Agree. We have made a revision for this throughout the manuscript.

- Variation of RI and RRCI are quite different for AK gauge station in Figure 6. Please state the reason

Response:

Thanks. For AK gauging station, there is a quite difference in the variation of RI and RRCI. This is because RRCI is dependent on both RI and the OR-joint exceedance probability (OR-JEP). As shown in Figure 2 (revised), in spite of a low value of RI, the MARI with a high OR-JEP value can get a high RRCI. In fact, the reservoir effect on the downstream flood is great under the condition of the fewer constraints (high OR-JEP values) from MARI. Thus, it is expected that RRCI can reflect a real reservoir effect more than RI.

- Uncertainty of flood estimates are greater in AK stations (Figure 8) compared to the others. The reason should be explained.

Response:

Thanks for this suggestion. The uncertainty range of AK station is larger than HJG and HZ stations. The possible explanation to the larger uncertainty range is that the sample size (1993-2015) of the regulated floods at AK station is smaller, and, furthermore, the dependent relationship between RRCI and AMDF at AK station is weaker. This explanation has been added in the revised manuscript.

- Discussion section is comparatively short to conclusion part. In general the paper describes a usable approach but the main weakness is insufficient discussion of the available results. I mean, it is stated that the downstream flood regime should be altered by upstream reservoirs and the magnitude of flood peaks are reduced due to the storage capacity of them. This is expected in such a reservoir system by analyzing long period AMDF values (see Figure 7, observed AMDF). Rather, the author should elaborately clarify GEV model results in Discussion part. Main results should be given under discussion, and conclusion should briefly summarize them. Considering these, I guess these two sections should be totally revised.

Response:

Thank you very much for this comment. Discussion and Conclusion have been totally revised. Discussion has been put in the Section 4.4 as follows:

4.4 Discussion

The long-term variation of the AMDF series (Figure 8) indicates that the upstream reservoirs have evidently altered the downstream flood regimes. As an example, since the completion of Danjiangkou reservoir in 1967, the flood magnitude of HZ station is evidently reduced overall. This is consistent with the results on the effects of reservoirs on the hydrological regime of this area in previous literature (Cong et al., 2013; GUO et al., 2008; Jiang et al., 2014; Lu et al., 2009). In this study, it is found that there is a significant difference between those downstream floods affected by the same reservoir system (with the same RI value). In most cases, relative small downstream floods were obtained. However, it is of interest to note that there still occurred unexpected large downstream floods in few cases, in spite of a large RI value. For example, most values of AMDF in HZ station are less 10000 m³/s since 1967, but the values of AMDF in 1983 and in 1975 are 25600 m³/s and 19900 m³/s, respectively. It is highlighted that those unexpected large downstream floods are probably related to the MARI effects on reservoir operation. The five largest (unexpected) floods since 1967 and the corresponding values of the scheduling-related MARI variables in the HZ station are shown in Table 8. It is found that the largest floods of 1967-2015 occurred in 1983. For this flood event, the MARI is a rare event (with the OR-JEP value of 0.435 ranking the second in 1967-2015) due to the largest mean intensity ($I = 20.2$ mm) and the second late occurrence ($T = 281$). Surprisingly, all the timing values of the MARI for these five unexpected downstream floods show the high rankings (2-9th). Those timing values are near the end (about the 300th day of the year) of the flood control period (July-October) in this area. Actually, near the end of the major flood control period, the storage capacity able to use should be decreased, because according to the operation rules of Danjiangkou reservoir (Zhang et al., 2009), there is a staged increasing flood limit water level in the flood control season. One important cause for those unexpected large downstream floods is probably that the remaining storage capacity at the end of flood season is not sufficient to reduce some late floods. Therefore, in addition to the own storage capacity of reservoirs, the MARI effects should be indispensably considered when attempting to accurately quantify the reservoir effects on downstream floods.

With the combination of both RI and OR-JEP, RRCI has a significant

difference from RI (Figure 6). With a few exceptions, RRCI values are higher than RI values. It is indicated that the real reservoir impact may be underestimated by RI in most cases. Moreover, RI will also probably overestimate the real reservoir impact in few cases, because of no considering some special rainfall events (i.e., the MARI with low values of OR-JEP). The results of the covariate-based nonstationary flood frequency analysis (Table 7, Figure 7 and Figure 8) demonstrate that compared to the RI-dependent scenario, the RRCI-dependent scenario for the optimal nonstationary distribution more completely captures the presence of nonstationarity in the downstream flood frequency. Therefore, RRCI might be a useful index in accessing the reservoir effects on the downstream flood frequency.

Finally, the estimation errors of OR-JEP should be noted. (1) Only those MARI samples which corresponds to the timing of AMDF are included to estimate OR-JEP; this means that some extreme MARI samples which corresponds to the non-maximum flow are not included, resulting in the estimation error for OR-JEP; to reduce this error, it might be worth considering the use of the peaks-over-threshold sampling method. (2) The areal-averaged MARI is based on the records of 16 rainfall stations with the IDW method; the estimation error of areal-averaged rainfall may be transferred to the OR-JEP estimation error; the additional rainfall site data and spatial distribution information are needed to reduce the OR-JEP estimation error. Nonetheless, the good performance of downstream flood frequency modeling demonstrates the MARI samples still remain representative in this study.

5 Conclusions

Accurately assessing the impact of reservoirs on downstream floods is an important issue for flood risk management. In this study, to evaluate the effects of reservoirs on downstream flood frequency of Hanjiang River, the rainfall-reservoir composite index (RRCI) is derived from the Eq. (2) which takes account of the combination of the reservoir index (RI) and the OR-joint exceedance probability (OR-JEP) of scheduling-related rainfall variables. The main findings are summarized as follows: (1) the magnitude of the downstream flood events has been reduced by the reservoir system in the study area; however, the long-term variation of the observed AMDF series show that despite of the large reservoirs, the unexpected large flood events still occurred several times, e.g., at Huangzhuang station in 1983; and one important cause for the unexpected large floods of Huangzhuang station may be

related to the operation strategy of staged increasing flood limit water level for Danjiangkou reservoir. (2) According to the results of the covariate-based nonstationary flood frequency analysis for each station, compared to the optimal RI-dependent distribution, the optimal RRCI-dependent distribution more completely captures the presence of nonstationarity in the downstream flood frequency. (3) Furthermore, in estimating 100-year return level for each station, the optimal RRCI-dependent distribution provides a lower 100-year return level but there exist exceptions, and provides a smaller uncertainty range associated with the uncertainty of model parameter.

Consequently, this study demonstrates the necessity of including the antecedent rainfall effects, in addition to the effects of reservoir storage capacity, on reservoir operation in assessing the reservoir effects on downstream flood frequency. The study might provide a comprehensive approach for the downstream flood risk management under the impacts of reservoirs.

- Figure and tables are appropriate. However, I have some doubts about the usefulness of Figure 9 to illustrate the reservoir effects on flood risk. It is not combining the results of the frequency model. It is not clear for what reason this figure stands for especially at the end of the result section. (I suggest removing this figure, as it is a bit confusing in terms of central theme of the paper). If authors would like to include it, I suggest them to re-organize its location through the manuscript and revise the descriptions to make it more clear (in Lines 387-395).

Response:

Agree. In order to highlight the central theme of the paper, Figure 9 has been deleted in the revised manuscript.

Specific comments:

-There are too much abbreviation in the manuscript. Maybe a glossary would be useful for the readers.

Response:

Thanks for this suggestion. In Supplementary Information, we have added a glossary for these abbreviations as follows:

Glossary and Notation:

$\alpha_0, \alpha_1, \beta_0, \beta_1$: parameters of nonstationary model.

A_i : total basin area upstream of the i -th reservoir.

A_T : total basin area upstream of the gauge station.
 AIC: Akaike information criterion.
 AK: Ankang (gauging station).
 AMDF: annual maximum daily flow (series).
 CDF: Cumulative distribution function
 d : dimension of copulas.
 df : freedom degree.
 GA: Gamma distribution
 GEV: Generalized Extreme Value distribution.
 GEV_S23: nonstationary GEV distribution with the S23 scenario.
 GML: generalized maximum likelihood (method).
 GU: Gumbel distribution.
 HJG: Huangjiagang (gauging station).
 HZ: Huang zhuang (gauging station).
 I : intensity, the mean of daily rainfall in MARI.
 IDW: Inverse distance weighting method.
 IRI: impounded runoff index, a ratio of reservoir capacity to mean annual runoff.
 \hat{l} : maximized likelihood of the model object.
 L : distance, the distance between the rainfall center and the outlet.
 LOGNO: Lognormal distribution.
 LR_i : loss rate (%) of total storage capacity of the i -th reservoir due to the sediment deposition.
 μ_t : mu parameter of the distribution functions used.
 M_c : length of the Markov chain.
 M : maximum, the maximum of daily rainfall in MARI.
 MARI: multiday antecedent rainfall input.
 MCMC: Markov chain Monte Carlo.
 ML: maximum likelihood (method).
 n : number of data points.
 N : total number of reservoirs upstream of the gauge station.
 OR-JEP: OR-joint exceedance probability.
 P_{MARI}^\vee : OR-joint exceedance probability.
 θ_i : parameter vector of the i -th marginal distribution.

θ_c : copula parameter vector.
 θ : parameter vector of the whole n -dimensional distribution.
 $\theta_{\text{GEV_S23}}$: parameters of the GEV_S23 model.
 $\hat{\theta}_{\text{GEV_S23}}^i$: an estimation for the parameters of the GEV_S23 model.
 \bar{Q} : mean annual runoff.
RRCI: rainfall-reservoir composite index.
RI: reservoir index.
RC: reservoir capacity.
 RC_i : total storage capacity of the i -th reservoir.
 σ_i : sigma parameter of the distribution functions used.
S0: constant scenario.
S1: RI-dependent scenarios.
S2: RRCI-dependent scenarios.
SBC: Schwarz Bayesian criterion.
 T : timing, the end time of MARI in the year.
 u_i : univariate marginal distribution of X_i .
 V : volume, the total of daily rainfall in MARI.
WEI: Weibull distribution.
 ξ : shape parameter of the Generalized Extreme Value distribution.
 X_1, X_2, \dots, X_d : scheduling-related MARI variables.

- Line 49, what is “nature extreme flow”?

Response:

For clarity, we have changed this sentence in the revised manuscript as follows:

In general, without reservoirs, the flood extremes downstream of most rain-dominated basins are mainly related to the extreme rainfall in the drainage area...

- Lines 50-52, what about the operational targets and other constraints?

Response:

Thanks. Our statement exists imprecise. We have rephrased it as follows:

However, with reservoirs, the downstream flood regimes should be totally different due to upstream flood control scheduling.

- Lines 52-54, requires more up-to-date references.

Response:

In the revision, we have added literature review on studies dealing with downstream hydrograph alterations caused by dams. Please see the response for “- Studies dealing with downstream hydrograph alterations caused by dams are not discussed enough in the literature.”.

- Lines 76-78, even a small reservoir could be very complex to derive operational strategies and a lot of detailed information might be required. I am not sure about this classification. Please consider revising this part.

Response:

Agree. A modification of this statement has been made as follows:

The continuous simulation method can explicitly account for the reservoir effects on flood in the hypothetical case. However, it is difficult to apply this approach to the most real cases (Volpi et al., 2018), because the simplifying assumptions of this approach are just satisfied in a few of basins with single small reservoir. Furthermore, even if the basins meet the simplifying assumptions, the detailed information required in this approach are probably unavailable.

- Line 96, what type of uncertainty?

Response:

The uncertainty of flood estimates is associated with the uncertainty of the parameters estimates. For clarity, we have revised this sentence as follows:

...Bayesian inference can get multiple estimates, forming a posterior distribution of model parameters. Thus, the Bayesian method is able to conveniently describe the uncertainty of flood estimates associated with the uncertainty of model parameters.

- Line 84, which “previous studies”?

Response:

Thanks. The correction has been made as follows:

Thus, previous studies (Adlouni et al., 2007; Ouarda and El - Adlouni, 2011) have used the nonstationary Generalized Extreme Value distribution (NGEV) to describe nonstationary maxima series.

- Line 108, it is a bit vague what do you mean by “more accurate effects of reservoirs?”

Response:

Thanks. For clarity, a modification of this sentence has been made as follows:

The precision and accuracy in the quantitative analysis of the reservoir effects on the downstream floods need to be improved further.

- Lines 115-117, please refer to Bayesian method in the objectives.

Response:

Agree. In the revision, Bayesian method has been referred in the objectives.

- Line 143, what do you mean by “more precise effects of reservoirs”?

Response:

Thanks. We have deleted this sentence.

- Line 146, please briefly explain “multiday rainfall input”.

Response:

Note that there is a modification of the name for MRI (revised as MARI) in the revised manuscript. In the revision, the brief explanation has been added as follows:

In addition to the reservoir capacity, multiday antecedent rainfall input (MARI), i.e., an event of the continuous multi-day multivariate rainfall forming the inflow event which will be regulated to become downstream extreme flow by the reservoir system is a key constraint for the scheduling of the reservoir system.

- Lines 147-150, It is a bit confusing whether scheduling related multivariate (SRMR) and MRI are same or not? Could you give more detail for their explanations.

Response:

Thanks.

SRMR and MRI are different. All variables of SRMR are selected from the variables of MRI. The SRMR variables is the scheduling related MARI variables. In the revised manuscript, for clarity, SRMR is deleted and MARI has been accurately described.

- Line 155, why OR-joint exceedance probability is selected as measure function?

Response:

We need a rainfall index to measure the effect of the antecedent rainfall on the reservoir operation. The OR-joint exceedance probability (OR-JEP) is the probability that any one of the given set of values (x_1, x_2, \dots, x_d) for the scheduling-related MARI variables will be exceeded. The lower this probability, the greater effects on reservoir operation the MARI has, and then, it is expected that the downstream floods possibly obtain relative large values. The above explanation has been added in the revised manuscript.

- Line 158, what do you mean by “reservoir scheduling is more inflexible”?

Response:

We realize that the word “inflexible” may be inappropriate. Here, what we want to express is that the reservoir scheduling will have more constraints from the MARI. For example, when MARI with a large volume occurs and its timing is near the end of flood season, the reservoir with a operation strategy of increasing flood limit water

level in stages will probably face a large peak of inflow and a insufficient residual capacity due to reservoir impounding. The above explanation will be added in the revised manuscript.

- Lines 170-172, selected four variables require more explanation.

Response:

Agree. The more detailed explanation has been added as follows:

In this study, to add the antecedent rainfall effects into the new indicator of reservoir effects, the five variables are considered to describe MARI, i.e., the maximum M (the maximum of daily rainfall in MARI), the intensity I (the mean of daily rainfall in MARI), the volume V (the total of daily rainfall in MARI), the timing T (the end time of MARI in the year) and the distance L (the distance between the rainfall center and the outlet). The reason that M , I , V , and L are selected is that these variables will determine the peak, the total volume and the peak appearance time of the inflow event. The variable T is utilized to capture the information of the remaining storage capacity, due to the staged operation strategies in the flood season for some reservoirs. For the operation strategy of increasing flood limit water level in stages, it is expected that if the timing of MARI is near the end of flood season, the downstream AMDF will be less affected by reservoirs, because of less remaining capacity in this period.

- Line 208, it is not clear “obeys nonstationary distribution”. Please revise.

Response:

The statement has been revised as follows:

Suppose that flood variable Y_t obeys distribution $f_Y(y_t|\boldsymbol{\eta}_t)$ with the distribution parameters $\boldsymbol{\eta}_t = [\mu_t, \sigma_t, \xi]$.

- Line 280-286. The sentence is too long and difficult to understand. Please separate and revise.

Response:

Thanks. The sentence has been separated and revised.

- Line 301, please revise “Actually, although: :”

Response:

Thanks. In the revision, this sentence has been deleted.

- Line 303-304, it is not clear what do you mean by “(e.g., special extreme MRI may limit or reduce the effects of the reservoir).”

Response:

In the revision, this sentence has been deleted.

- Line 314-315, please describe and relate calculated Spearman correlations in the text, otherwise remove them.

Response:

The description and relation for the calculated Spearman correlations has been added in the revised text.

-Lines 338-339, please clarify “special rainfall events”

Response:

In the revision, this phrase has been deleted.

- Lines 412-413, please mention future studies in Conclusion part, not under Discussion.

Response:

In the revision, we have followed your suggestion.

- Line 429, it is not clear what do you mean by “some rare multivariate MRI still would produce lower values of RRCI than that of RI”. Please revise it.

Response:

Thanks. This sentence has been revised in the revised manuscript.

Technical corrections:

- Figure 1. The caption should be “The flowchart of nonstationary covariate-based flood frequency analysis with a rainfall-reservoir composite index (RRCI)

Response:

Thank you for this comment. We have revised the caption according to your suggestion.

- Figure 7. In the caption, “thick blue” should be “thick blue line”.

Response:

Corrected.

- Table 2. It would be better to not to duplicate “Dangjiangkou reservoir” and remove first row. The details should be given in the text only.

Response:

Corrected.

- Line 26, please revise “of the previous study”

Response:

Revised.

- Line 35, please revise “What’s more”

Response:

Revised.

- Lines 62-63, please revise the sentence.

Response:

Revised.

– In Line 73, it is stated three model components but not clear which of them are ordered since only two are given?

Response:

Thanks. This is a mistake. We have corrected this sentence as follows:

... In the first approach, the regulated flood time series can be simulated by using three model components, i.e., the stochastic rainfall generator, the rainfall-runoff model and the reservoir flood operation module which includes the reservoir storage capacity, the size of release structures and the operation rules....

- Line 76-78, too long sentence and hard to follow. Please revise it.

Response:

Thanks. We have revised this sentence. Please see the response for “- Lines 76-78, even a small reservoir could be very complex...”

- Line 119, please explain AMDF.

Response:

The explanation has been added in the revision as follows:

To quantify the effects of reservoirs on the frequency of the annual maximum daily flow series (AMDF) downstream of reservoirs,...

- Line 114 and Line 120, “RRIC” should be “RRCT”

Response:

Corrected.

- Line 115, “to calculate” should be replaced with “to develop”

Response:

Corrected.

- Line 139, “the Eq. (1)” should be replaced with “Eq. (1)”

Response:

Corrected.

1 **Assessing the impacts of reservoirs on the downstream flood frequency by coupling**
2 **the effect of the scheduling-related multivariate rainfall into an indicator of**
3 **reservoir effects**

4 Bin Xiong¹, Lihua Xiong^{1*}, Jun Xia¹, Chong-Yu Xu^{1,3}, Cong Jiang², Tao Du⁴

5 1. State Key Laboratory of Water Resources and Hydropower Engineering Science, Wuhan
6 University, Wuhan 430072, China

7 2. School of Environmental Studies, China University of Geosciences, Wuhan 430074, China

8 3. Department of Geosciences, University of Oslo, P.O. Box 1022 Blindern, N-0315 Oslo, Norway

9 4. Bureau of Hydrology, Changjiang Water Resources Commission, Wuhan 430010, China

10
11 * *Corresponding author:*

12 Lihua Xiong, PhD, Professor

13 State Key Laboratory of Water Resources and Hydropower Engineering Science

14 Wuhan University, Wuhan 430072, China

15 E-mail: xionglh@whu.edu.cn

16 Telephone: +86-13871078660

17 Fax: +86-27-68773568

18

19 **Abstract:**

20 Many studies have shown that the downstream flood regimes have been significantly altered by
21 upstream reservoir operation. Reservoir effects on the downstream flow regime are normally carried out
22 by comparing the pre-dam and post-dam frequencies of some streamflow indicators such as floods and
23 droughts. In this paper, a rainfall-reservoir composite index (RRCI) is developed to precisely quantify
24 reservoir impacts on downstream flood frequency under a framework of the covariate-based
25 nonstationary flood frequency analysis with Bayesian inference method. The RRCI is derived from the
26 combination of both a reservoir index (RI) for measuring the effects of reservoir storage capacity and a
27 rainfall index, i.e., the OR-joint exceedance probability (OR-JEP) of some scheduling-related variables
28 selected out of the five variables describing multiday antecedent rainfall input (MARI), for measuring
29 the effects of antecedent rainfall on reservoir operation. Then, with RI-dependent or RRCI-dependent
30 distribution parameters, five distributions, i.e., Gamma, Weibull, Lognormal, Gumbel and Generalized
31 Extreme Value, are used to analyze the annual maximum daily flow (AMDF) of Ankang, Huangjiagang
32 and Huangzhuang gauging stations of Hanjiang River, China. A phenomenon is observed that although
33 most flood peaks downstream of reservoirs had been reduced in magnitude by the upstream reservoirs,
34 some relatively large flood events still occurred several times, e.g., at the Huangzhuang station in 1983.
35 The results of nonstationary flood frequency analysis show that, in comparison to RI, RRCI that
36 combines both RI and OR-JEP can make a much better explanation for such a phenomenon of the flood

occurrences downstream of reservoirs. Bayesian inference of the 100-year return level of AMDF shows that the optimal RRCI-dependent distribution, compared to the RI-dependent one, gives relative smaller estimate values but there exist exceptions due to some low OR-JEP values, and provides a smaller uncertainty range. This study highlights the necessity of including the antecedent rainfall effects, in addition to the effects of reservoir storage capacity, on reservoir operation in assessing the reservoir effects on downstream flood frequency. This analysis might provide a more comprehensive approach for downstream flood risk management under the impacts of reservoirs.

Keywords: Nonstationary flood frequency analysis; downstream floods; reservoir; antecedent rainfall; Bayesian inference; Hanjiang River

1 Introduction

River floods are generated by various complex nonlinear processes involving physical factors including “hydrological pre-conditions (e.g. soil saturation, snow cover), meteorological conditions (e.g. amount, intensity, and spatial and temporal distribution of rainfall), runoff generation processes as well as river routing (e.g. superposition of flood waves in the main river and its tributaries)” (Wyżga et al., 2016). In general, without reservoirs, the flood extremes downstream of most rain-dominated basins are mainly related to the extreme rainfall in the drainage area. However, with reservoirs, the downstream flood regimes should be totally different due to upstream flood control scheduling. In the literature, the significant hydrological alterations caused by reservoirs are demonstrated in the many areas of the

world. Graf (1999) showed that the dams have greater effects on the streamflow than the global climate change in America. Benito and Thorndycraft (2005) reported various significant changes of the pre- and post-dam hydrologic regimes (e.g., minimum and maximum flows over different durations) across the United States. Batalla et al. (2004) demonstrated an evident reservoir-induced hydrologic alteration in the North-Eastern Spain. Yang et al. (2008) indicated the spatial variability of the hydrological regimes alteration caused by the reservoirs in the middle and lower Yellow River, China. Mei et al. (2015) found that the Three Gorges Dam, the largest dam in the world, has significantly changed the downstream hydrological regimes. In recent years, the cause-effect mechanisms of the downstream flood peak reduction were also investigated in some literature (Ayalew et al., 2013; 2015; Volpi et al., 2018). For example, Volpi et al. (2018) suggested that for a single reservoir, the downstream flood peak reduction is mainly dependent on its position along the river, its spillway and its storage capacity based on a parsimonious instantaneous unit hydrograph-based model. These studies have revealed that it is crucial to assess the impacts of reservoirs on downstream flood regimes for the success of downstream flood risk management.

Flood frequency analysis is the most common technique used by hydrologists to gain knowledge of flood regimes. For conventional or stationary frequency analysis, a basic hypothesis is that hydrologic time series keeps stationarity, i.e., “free of trends, shifts or periodicity (cyclicality)” (Salas, 1993). However, in many cases, the change of flood regime has demonstrated that this strict assumption

73 is invalid (Kwon et al., 2008; Milly et al., 2008). Nonstationarity in the flood regime downstream of
74 dams makes frequency analysis more complicate. Actually, the frequency of floods downstream of
75 dams is closely related to upstream flood operation. In recent years, there are a lot of attempts linking
76 flood generating mechanisms and reservoir operation to the frequency of downstream floods (Gilroy
77 and Mccuen, 2012; Goel et al., 1997; Lee et al., 2017; Liang et al., 2017; Su and Chen, 2018; Yan et al.,
78 2017).

79 Previous studies have meaningfully increased the knowledge about the reservoir-induced
80 nonstationarity of downstream hydrological extreme frequency (Ayalew et al., 2013; L ópez and Franc és,
81 2013; Liang et al., 2017; Magilligan and Nislow, 2005; Su and Chen, 2018; Wang et al., 2017; Zhang et
82 al., 2015). There are two main approaches to incorporate reservoir effects into flood frequency analysis:
83 the hydrological model simulation approach and the nonstationary frequency modeling approach. In the
84 first approach, the regulated flood time series can be simulated by using three model components, i.e.,
85 the stochastic rainfall generator, the rainfall-runoff model and the reservoir flood operation module
86 which includes the reservoir storage capacity, the size of release structures and the operation rules. The
87 continuous simulation method can explicitly account for the reservoir effects on flood in the
88 hypothetical case. However, it is difficult to apply this approach to the most real cases (Volpi et al.,
89 2018), because the simplifying assumptions of this approach are just satisfied in a few of basins with
90 single small reservoir. Furthermore, even if the basins meet the simplifying assumptions, the detailed

91 information required in this approach are probably unavailable. Thus, our attention is focused on the
92 second method, the nonstationary frequency modeling approach. Nonstationary distribution models
93 have been widely used to deal with the nonstationarity of extreme values series. In nonstationary
94 distribution models, distribution parameters are expressed as the functions of covariates to determine
95 the conditional distributions of the extreme values series. According to extreme value theory, the
96 maxima series can generally be described by the Generalized Extreme Value distribution (GEV). Thus,
97 previous studies (Adlouni et al., 2007; Ouarda and El - Adlouni, 2011) have used the nonstationary
98 Generalized Extreme Value distribution to describe nonstationary maxima series. Scarf (1992) modeled
99 the change in the location and scale parameters of GEV over time through the power function
100 relationship. Coles (2001) introduced several time-dependent structures (e.g., trend, quadratic and
101 change-point) into the location, scale and shape parameters of GEV. Adlouni et al. (2007) provided a
102 general nonstationary GEV model with an improved parameter estimate method. In recent years,
103 “generalized additive models for location, scale and shape” (GAMLSS) was widely used in
104 nonstationary hydrological frequency analysis (Du et al., 2015; Jiang et al., 2014; López and Francés,
105 2013; Rigby and Stasinopoulos, 2005; Villarini et al., 2009). GAMLSS provides various candidate
106 distributions for frequency analysis, e.g., Weibull, Gamma, Gumbel, and Lognormal distributions.
107 However, GEV is rarely involved in the candidate distributions of GAMLSS. In terms of the parameter
108 estimation method for the nonstationary distribution model, the maximum likelihood (ML) method is

109 the most common parameter estimate method. However, the ML method for the nonstationary
110 distribution model may diverge when using numerical techniques to solve the likelihood function with
111 the small sample. Another drawback of the ML method is its inconvenience to describe the uncertainty
112 of model parameters estimates, because the ML can only get one estimate of the model parameters
113 through maximization of the likelihood function. Adlouni et al. (2007) developed the generalized
114 maximum likelihood (GML) method and demonstrated that the GML method has better performance
115 than the ML method in all their cases. Ouarda and El - Adlouni (2011) introduced the Bayesian
116 nonstationary frequency analysis. The Bayesian inference can get multiple estimates, forming a
117 posterior distribution of model parameters. Thus, the Bayesian method is able to conveniently describe
118 the uncertainty of flood estimates associated with the uncertainty of model parameters.

119 In the nonstationary frequency modeling approach, a dimensionless reservoir index (RI), as an
120 indicator of reservoir effects, was proposed by López and Francés (2013), and it generally is used as
121 covariate for the expression of the distribution parameters (e.g., location parameter) (Jiang et al., 2014;
122 López and Francés, 2013). Liang et al. (2017) modified the reservoir index by replacing the mean
123 annual runoff in the expression of RI with the annual runoff, so that the modified reservoir index can
124 reflect the impact of reservoirs on downstream flood extremes under different total inflow conditions
125 each year. However, the precision and accuracy in the quantitative analysis of the reservoir effects on
126 the downstream floods need to be improved further.. In fact, the effects of reservoirs may be closely

127 related not only to the static reservoir storage capacity, but also to the dynamic reservoir operation
128 associated with the multiple characteristics (e.g., the peak, the intensity and the total volume) of the
129 multiday antecedent rainfall input (MARI), not just annual runoff.

130 Therefore, the aim of the study is to develop an indicator named the rainfall-reservoir composite
131 index (RRIC) combining the effects of reservoir storage capacity and MARI on reservoir operation, and
132 then to utilize this indicator as covariate to assess the reservoir effects on the downstream flood
133 frequency. The specific objectives of this study are: (1) to develop RRIC; (2) to compare RRIC with RI
134 through the covariate-based nonstationary flood frequency analysis; and (3) to obtain the downstream
135 flood estimation and its uncertainty based on the optimal nonstationary distribution with Bayesian
136 inference.

137 2 Methods

138 To quantify the effects of reservoirs on the frequency of the annual maximum daily flow series
139 (AMDF) downstream of reservoirs, a three-step framework (Figure 1), termed the covariate-based flood
140 frequency analysis using RRIC as covariate, is established. In this section, the methods in this
141 framework are introduced. First, a reservoir index (RI) is defined with additionally considering the
142 effects of reservoir sediment deposition on the storage capacity. Second, RRIC is developed through
143 combining RI and a rainfall index. And then, the C-vine copula model is used to construct to calculate

the rainfall index. Fourth and last, the nonstationary distribution models with the Bayesian estimation are clarified.

<Figure 1>

2.1 Reservoir index (RI)

Intuitively, the larger the reservoir capacity relative to the flow of a downstream gauging station, the greater the effects of reservoir on the streamflow regime are possible. To quantify the reservoir-induced alteration to the downstream streamflow regime, Batalla et al. (2004) proposed the impounded runoff index (IRI), a ratio of reservoir capacity (RC) to (unimpaired) mean annual runoff (\bar{Q}) at the gauge station, indicated as $IRI = RC/\bar{Q}$. For single reservoir, the IRI is a good indicator of the extent to which the reservoir alters streamflow. To analyze the effects of multi-reservoir system on the downstream flood frequency, López and Francés (2013) proposed a dimensionless reservoir index. In this study, we additionally consider the effects of reservoir sediment deposition on the reservoir capacity. Following López and Francés (2013), the reservoir index (RI) for a downstream gauging station is defined as

$$RI = \sum_{i=1}^N \left(\frac{A_i}{A_T} \right) \cdot \left(\frac{(1 - LR_i) \cdot RC_i}{\bar{Q}} \right) \quad (1)$$

where N is the total number of reservoirs upstream of the gauge station, A_i is the total basin area upstream of the i -th reservoir, A_T is the total basin area upstream of the gauge station, RC_i is the total

161 storage capacity of the i -th reservoir, LR_i is the loss rate (%) of RC_i due to the sediment deposition
162 (Appendix A). The Eq. (1) indicates that for the reservoir system consisting of small and middle sized
163 reservoirs, RI for the downstream gauging station is generally less than 1, but for the system with some
164 large reservoirs, e.g., multi-year regulating storage reservoirs, RI of the downstream gauging station
165 near this system may be close to 1 or higher.

166 2.2 Rainfall-reservoir composite index (RRCI)

167 In addition to the reservoir capacity, multiday antecedent rainfall input (MARI), i.e., an event of
168 the continuous multi-day multivariate rainfall forming the inflow event which will be regulated to
169 become downstream extreme flow by the reservoir system is a key constraint for the scheduling of the
170 reservoir system. In this study, to add the antecedent rainfall effects into the new indicator of reservoir
171 effects, the five variables are considered to describe MARI, i.e., the maximum M (the maximum of
172 daily rainfall in MARI), the intensity I (the mean of daily rainfall in MARI), the volume V (the total of
173 daily rainfall in MARI), the timing T (the end time of MARI in the year) and the distance L (the
174 distance between the rainfall center and the outlet). The reason that M , I , V , and L are selected is that
175 these variables will determine the peak, the total volume and the peak appearance time of the inflow
176 event. The variable T is utilized to capture the information of the remaining storage capacity, due to the
177 staged operation strategies in the flood season for some reservoirs. For the operation strategy of

increasing flood limit water level in stages, it is expected that if the timing of MARI is near the end of flood season, the downstream AMDF will be less affected by reservoirs, because of less remaining capacity in this period. Those MARI variables which are selected to construct the new indicator are referred to as the scheduling-related MARI variables (denoted as X_1, X_2, \dots, X_d), hereafter. The extraction procedure of the MARI is detailed in the section 3.2.

We propose the new index called rainfall-reservoir composite index (RRCI) for more comprehensively assessing effects of reservoirs on floods by incorporating the effects of MARI, defined as

$$\text{RRCI} = \begin{cases} \left(P_{\text{MARI}}^{\vee} \left(\bigcup_{i=1}^d (X_i > x_i) \right) \right)^{(1/\text{RI}-1)}, & 0 < \text{RI} \leq 1 \\ \text{RI}, & \text{RI} > 1 \end{cases} \quad (2)$$

where P_{MARI}^{\vee} is the OR-joint exceedance probability (OR-JEP), i.e., the probability that any one of the given set of values (x_1, x_2, \dots, x_d) for the scheduling-related MARI variables will be exceeded. Here, OR-JEP acts as the rainfall index of measuring the MARI effects. The lower this probability, the greater effects on reservoir operation the MARI has, and then, it is expected that the downstream floods possibly obtain relative large values, and vice versa. Figure 2 illustrates the relationship in the Eq. (2), which shows that RRCI is conditional on both OR-JEP and RI. The Eq. (2) can be expressed as

$$\text{RRCI} = \begin{cases} \left(1 - F(x_1, x_2, \dots, x_d) \right)^{(1/\text{RI}-1)}, & 0 < \text{RI} \leq 1 \\ \text{RI}, & \text{RI} > 1 \end{cases} \quad (3)$$

where $F(\cdot)$ is the cumulative distribution function (CDF), determining the dependence relationship of the variables. The expectation of RRCI is as follow

$$E(\text{RRCI}) = \int_{\mathbb{R}^d} (1 - F(x_1, x_2, \dots, x_d))^{(1/\text{RI}-1)} dF(x_1, x_2, \dots, x_d) = \text{RI} \quad (4)$$

In addition, for the OR case, we have

$$P_{\text{MARI}}^\vee \left(\bigcup_{i=1}^d (X_i > x_i) \right) \geq P_{\text{MARI}}^\vee (X_i > x_i) \quad (5)$$

The Eq. (3) and Eq. (5) indicate that in addition to RI, RRCI is related to the number and the dependence relationship of the scheduling-related MARI variables. To give a reasonable RRCI, the unrelated MARI variables should not be incorporated. In this study, the number of MARI variables to be incorporated is no more than four to avoid "dimension disaster" in modeling their dependence. To select the scheduling-related MARI variables, the three-step selection procedure includes (1) selecting four variables from the five MARI variables through testing the significance of the Pearson correlation between the MARI variables and AMDF, (2) calculating RRCI for all the possible subsets of the four variables through the d -dimensional ($d = 1, 2, 3, 4$) copulas, and (3) identifying the variables through the highest rank correlation coefficient between RRCI and AMDF. The construction method of d -dimensional ($d = 2, 3, 4$) distribution $F(x_1, x_2, \dots, x_d)$ is described in the following subsection.

<Figure 2>

210 2.3 C-vine Copula model

211 In this subsection, a c-vine Copula model for the construction of continuous d -dimensional
212 distribution $F(x_1, x_2, \dots, x_d)$ is clarified. The Sklar's theorem (Sklar, 1959) showed that for a continuous
213 d -dimensional distribution, one-dimensional marginals and dependence structure can be separated, and
214 the dependence can be represented by a copula formula as follows

$$215 \quad F(x_1, x_2, \dots, x_d | \boldsymbol{\theta}) = C(u_1, u_2, \dots, u_d | \boldsymbol{\theta}_c), u_i = F_{x_i}(x_i | \boldsymbol{\theta}_i) \quad (6)$$

216 where u_i is the univariate marginal distribution of X_i ; $C(\cdot)$ is the copula function. $\boldsymbol{\theta}_c$ is the copula
217 parameter vector; $\boldsymbol{\theta}_i$ is the parameter vector of the i -th marginal distribution. $\boldsymbol{\theta} = (\boldsymbol{\theta}_c, \boldsymbol{\theta}_1, \boldsymbol{\theta}_2, \dots, \boldsymbol{\theta}_d)$ is the
218 parameter vector of the whole n -dimensional distribution. Thus, the construction of $F(x_1, x_2, \dots, x_d)$ can
219 be separated into two steps: first is the modeling of the univariate marginals; second is the modeling of
220 the dependence structure. For the first step, we use the empirical distribution as univariate marginal
221 distributions and the change-points of the variables are tested by the Pettitt test (Pettitt, 1979), and then,
222 if any, the marginal with the change-point will be addressed by the estimation method (Xiong et al.,
223 2015). Then, for the second step, the copula construction for the dependence modeling is based on the
224 pair-copula construction method which has been widely used in the previous research (Aas et al., 2009;
225 Xiong et al., 2015). According to Aas et al. (2009), the joint density function $f(x_1, x_2, \dots, x_d)$ is written
226 as

$$f(x_1, x_2, \dots, x_d | \boldsymbol{\theta}) = c_{1\dots n}(u_1, u_2, \dots, u_d | \boldsymbol{\theta}_c) \prod_{i=1}^d f_{x_i}(x_i | \boldsymbol{\theta}_i), u_i = F_{x_i}(x_i | \boldsymbol{\theta}_i) \quad (7)$$

and the n -dimensional copula density $c_{1\dots d}(u_1, u_2, \dots, u_d)$, which can be decomposed into $d(d-1)/2$

bivariate copulas, corresponding to a c-vine structure, is given by

$$c_{1\dots d}(u_1, u_2, \dots, u_d | \boldsymbol{\theta}_c) = \prod_{j=1}^{d-1} \prod_{i=1}^{d-j} c_{j,i+j|1,\dots,j-1} \left(F(u_j | u_1, \dots, u_{j-1}), F(u_{i+j} | u_1, \dots, u_{j-1}) | \boldsymbol{\theta}_{j,i|1,\dots,j-1} \right) \quad (8)$$

where $c_{j,i+j|1,\dots,j-1}$ is the density function of a bivariate pair copula and $\boldsymbol{\theta}_{j,i|1,\dots,j-1}$ is a parameter vector of

the corresponding bivariate pair copula. And the marginal conditional distribution is

$$F(u_{i+j} | u_1, \dots, u_{j-1}) = \frac{\partial C_{i+j,j-1|1,\dots,j-2} \left(F(u_{i+j} | u_1, \dots, u_{j-2}), F(u_{j-1} | u_1, \dots, u_{j-2}) | \boldsymbol{\theta}_{i+j,j-1|1,\dots,j-2} \right)}{\partial F(u_{j-1} | u_1, \dots, u_{j-2})}, \quad (9)$$

$j = 2, \dots, d-1; i = 0, \dots, n-j$

where $C_{i+j,j-1|1,\dots,j-2}$ is a bivariate copula distribution function. The maximum dimensionality covered in

this study is four. Thus for the four-dimensional copula (of which the decomposition is shown in Figure

3), the general expression of Eq. (8) is

$$c_{1234}(u_1, u_2, u_3, u_4 | \boldsymbol{\theta}_c) = c_{12}(u_1, u_2 | \boldsymbol{\theta}_{12}) c_{13}(u_1, u_3 | \boldsymbol{\theta}_{13}) c_{14}(u_1, u_4 | \boldsymbol{\theta}_{14}) \cdot c_{23|1} \left(F(u_2 | u_1), F(u_3 | u_1) | \boldsymbol{\theta}_{23|1} \right) c_{24|1} \left(F(u_2 | u_1), F(u_4 | u_1) | \boldsymbol{\theta}_{24|1} \right) \cdot c_{34|12} \left(F(u_3 | u_1, u_2), F(u_4 | u_1, u_2) | \boldsymbol{\theta}_{34|12} \right) \quad (10)$$

<Figure 3>

239 **2.4 Covariate-based nonstationary frequency analysis with Bayesian estimation**

240 The covariate-based extreme frequency analysis has been widely used (Villarini et al., 2009;
241 Ouarda and El - Adlouni, 2011; López and Francés, 2013; Xiong et al., 2018). Following these studies,
242 five distributions, i.e., Gamma (GA), Weibull (WEI), Lognormal (LOGNO), Gumbel (GU) and
243 Generalized Extreme Value (GEV), are used as candidate distributions in this study. And their density
244 functions, the corresponding moments and the used link functions are shown in Table 1. In the
245 following, the nonstationary distribution models based on Bayesian estimation are developed for
246 covariate-based flood frequency analysis.

247 <Table 1>

248 Suppose that flood variable Y_t obeys distribution $f_{Y_t}(y_t|\boldsymbol{\eta}_t)$ with the distribution parameters
249 $\boldsymbol{\eta}_t = [\mu_t, \sigma_t, \xi]$. In this study, only distribution parameters μ_t and σ_t are allowed to be dependent on
250 covariates, with considering that the shape parameter ξ of GEV is sensitive to quantile estimation of
251 rare events. According to the linear additive formulation of Generalized Additive Models for Location,
252 Scale, and Shape (GAMLSS) (Rigby and Stasinopoulos, 2005; Villarini et al., 2009), seven
253 nonstationary scenarios for the formulas of the two distribution parameters μ_t and σ_t are investigated, as
254 shown in Table 2. The constant scenario (S0) includes one scenario (both μ_t and σ_t are constants). The
255 RI-dependent scenarios (S1) include three scenarios, i.e., S11 (μ_t is RI-dependent and σ_t is constant),

S12 (μ_t is constant and σ_t is RI-dependent) and S13 (both μ_t and σ_t are RI-dependent). And the RRCI-dependent scenarios (S2) include S21, S22 and S23 as similar as S11, S12 and S13, respectively.

<Table 2>

In the following, Bayesian inference is introduced. Take GEV_S23 (representing the nonstationary GEV distribution with the S23 scenario) model as an example, the model parameter vector $\boldsymbol{\theta}_{\text{GEV_S23}} = [\alpha_0, \alpha_1, \beta_0, \beta_1, \xi]$ is to be estimate. We use the Bayesian method to estimate $\boldsymbol{\theta}_{\text{GEV_S23}}$. Let the prior probability distribution be $\pi(\boldsymbol{\theta}_{\text{GEV_S23}})$ and observations \mathbf{D} have the likelihood $l(\mathbf{D}|\boldsymbol{\theta}_{\text{GEV_S23}})$, then the posterior probability distribution $p(\boldsymbol{\theta}_{\text{GEV_S23}}|\mathbf{D})$ can be calculated with Bayes' theorem, as follow

$$p(\boldsymbol{\theta}_{\text{GEV_S23}}|\mathbf{D}) = \frac{l(\mathbf{D}|\boldsymbol{\theta}_{\text{GEV_S23}})\pi(\boldsymbol{\theta}_{\text{GEV_S23}})}{\int_{\Omega} l(\mathbf{D}|\boldsymbol{\theta}_{\text{GEV_S23}})\pi(\boldsymbol{\theta}_{\text{GEV_S23}})d\boldsymbol{\theta}_{\text{GEV_S23}}} \propto l(\mathbf{D}|\boldsymbol{\theta}_{\text{GEV_S23}})\pi(\boldsymbol{\theta}_{\text{GEV_S23}}) \quad (11)$$

where the integral is the normalizing constant and Ω is the whole parameter space. The obvious difference between the Bayesian method and the frequentist method is that the Bayesian method considers the parameters $\boldsymbol{\theta}_{\text{GEV_S23}}$ to be random variables, and the desired distribution of the random variables can be obtained by a Markov chain which can constructed by using various Markov chain Monte Carlo (MCMC) algorithms (Reis Jr and Stedinger, 2005; Ribatet et al., 2007) to process Eq. (11). And in this study, we use the Metropolis-Hastings algorithm (Chib and Greenberg, 1995; Viglione et al., 2013), which can be done by aid of the R package “MHadaptive” (Chivers, 2012). We use a beta

273 distribution function with the parameters $u = 6$ and $v = 9$, which is suggested by Martins and Stedinger
 274 (2000); Martins and Stedinger (2001), as the prior distribution on the shape parameter ξ . For the other
 275 **model** parameters $\alpha_0, \alpha_1, \beta_0, \beta_1$, the prior distributions are set to non-informative (flat) priors. There are
 276 two advantage of the Bayesian method. First, as noted by Adlouni et al. (2007), this method allows the
 277 addition of the other information, e.g., historical and regional information, through defining the prior
 278 distribution. Second, the Bayesian method can provide an explicit way to account for the uncertainty of
 279 **parameters estimates**. In nonstationary case, in the t -year, the 95% credible interval for the estimation of
 280 the flood quantile corresponding to a given probability P can be obtained from a set of stable
 281 parameters estimations $\hat{\theta}_{\text{GEV}_{S23}}^i (i = 1, 2, \dots, M_c)$ in which M_c is the length of the Markov chain.

282 **The procedure of model selection can identify which of the five distributions is optimal, which**
 283 **of the seven nonstationary scenarios is optimal. If all the distribution parameters are identified as**
 284 **constants (S0), this process will be the stationary frequency analysis. To select the optimal model, the**
 285 **Schwarz Bayesian criterion (SBC) (Schwarz, 1978) for each fitted model object is calculated by**

$$286 \quad \text{SBC} = -2 \ln(\hat{l}) + \ln(n) * \text{df} \quad (12)$$

287 **where $\ln(\hat{l})$ is the maximized log-likelihood of the model object, df is the freedom degree and n is the**
 288 **number of data points. SBC has a larger penalty on the over-fitting phenomenon than Akaike**
 289 **information criterion (AIC) (Akaike, 1974). The model object with the lower SBC is preferred. The**
 290 **worm plot and the QQ plot are employed to check whether the model can well represent the data.**

291 **3 Study area and data**

292 **3.1 Study area**

293 Hanjiang River (Figure 4), with the coordinates of 30°30'-34°30' N, 106°00'-114°00' E and a
294 catchment area of 159000 km², is the largest tributary of the Yangtze River, China. This area has a
295 warm temperate, semi-humid, continental monsoon climate. The temperature in the basin is not much
296 different from upstream to downstream. Although the elevation range of the study area is quite wide
297 (13–3493 m), the study area is a rainfall-dominated area and the snowmelt contribution is quite limited.
298 Take Ankang gauging station as an example. The timing of AMDF is mainly during the major rainfall
299 period from June to September (Figure S3a, c and d). And the winter is warm with the mean
300 temperature values of more than 2 °C as shown in Figure S3b. Since 1960, many reservoirs have been
301 completed in Hanjiang basin. The information of the five major reservoirs has been shown in Table 3,
302 including the longitude, latitude, control area, time for completion and capability. The Danjiangkou
303 Reservoir in central China's Hubei province is the largest one in this basin, and was completed by 1967.
304 As a multi-purpose reservoir, it mainly aims to supply water and control floods, and is also used for
305 electricity generation and irrigation. The reservoir has the total storage capacity of 21.0 billion m³, the
306 dead storage capacity of 7.23 billion m³, the effective storage capacity of 10.2 billion m³, and the flood
307 control capacity of 7.72 billion m³. After the Danjiangkou Dam Extension Project in 2010, the

308 Danjiangkou Reservoir gained an additional capacity of 13.0 billion m³ and an extra flood control
309 storage capacity of 3.3 billion m³. Besides, this reservoir is operated by the strategy of staged increasing
310 flood limit water level in the flood control season (Zhang et al., 2009).

311 <Figure 4>

312 <Table 3>

313 **3.2 Data**

314 The assessment analysis of reservoir effects on flood frequency utilizes the streamflow data, the
315 reservoir data, and the rainfall data. The annual maximum daily flood series (AMDF) is extracted from
316 the daily streamflow records of the three gauges in Hanjiang River basin, namely Ankang (AK) station
317 with a drainage area of 38600 km², Huangjiagang (HJG) station with a drainage area of 90491 km² and
318 Huangzhuang (HZ) station with a drainage area of 142056 km². The streamflow and reservoir data are
319 provided by the Hydrology Bureau of the Changjiang Water Resources Commission, China
320 (<http://www.cjh.com.cn/en/index.html>). The annual series of the maximum (M), the intensity (I),
321 volume (V), the timing (T) and the distance (L) are extracted from the daily streamflow data to
322 describe the MARI. Note that the timing of MARI is equal to the occurrence time of AMDF in the year,
323 MARI is an areal-averaged event, and any two consecutive days of areal rainfall values in MARI
324 require more than 0.2 mm. Daily areal rainfall is calculated using the inverse distance weighting (IDW)

method, based on the rainfall records of 16 stations (shown in Figure 4). These rainfall data are downloaded from the National Climate Center of the China Meteorological Administration (source: <http://www.cma.gov.cn/>). For AK and HZ gauging stations, all records are available from 1956 to 2015, while the records of HJG gauging station are available from 1956 to 2013.

4 Results and discussion

4.1 Identification of reservoir effects

In order to confirm the impact of reservoirs on annual maximum daily flow (AMDF) in the study area, the mean and standard deviation of AMDF before and after the construction of the two large reservoirs, i.e., the Danjiangkou reservoir (1967) upstream of HJG and HZ stations and the Ankang reservoir (1992) upstream of AK, HJG and HZ stations, are compared. According to the Table 4, the mean and standard deviation of AMDF in AK, HJG and HZ stations has been significantly reduced. Taking the HJG station as an example, the mean of AMDF (1992-2013) is 4139 m³/s, which is only 0.28 time of 14951 m³/s (1956-1966) and the standard deviation is 4074 m³/s, about 0.52 time of 7896 m³/s (1956-1966).

<Table 4>

Figure 5 presents the linear correlation between the five MARI variables (i.e., the maximum, M ; the intensity, I ; volume, V ; the timing, T ; and the distance L) and AMDF. It is found that for M , I , V and T , except for T in AK station, the Pearson correlation coefficients between those four variables and AMDF range from 0.27 to 0.71 (p-value>0.05), indicating that those four variables are significantly

344 related to AMDF. However, there is a Pearson correlation coefficient of no more than 0.24 between L
345 and AMDF for each stations, indicating that the location of rainfall may not be significantly related to
346 AMDF of the outlet. Thus, L is excluded for the calculation of RRCI. The further analysis for the
347 reservoir effects on downstream AMDF is performed in the following sections.

348 <Figure 5>

349 **4.2 Results for rainfall-reservoir composite index (RRCI)**

350 To obtain the annual values of RRCI, RI is estimated firstly. RI is affected by the loss of the
351 reservoir capacity but not too much (Figure S2), because the main reservoirs (i.e., Dangjiangkou and
352 Ankang reservoirs) have a small loss rate no more than 15% (Table S1 and Figure S1).

353 The C-vine copula model is applied to calculate OR-JEP of the scheduling-related MARI
354 variables. In the modeling of the univariate marginal, the marginals of the intensity (I) of AK and HJG
355 stations and the volume (V) of the HJG station are revised to deal with their significant change-points
356 (Table S2). To identify the scheduling-related variables from M , I , V , and T , RRCI for all the possible
357 subsets of M , I , V , and T is calculated and compared. The Pearson, Kendall, and Spearman correlation
358 coefficients between RRCI and AMDF are listed in Table 5. Note that the whole decomposition
359 structure of the C-vine copula for each RRCI of the same station is determined by the ordering of the
360 variables of each subset (shown in the cells of the first column of Table 5). Figure 3 is an example for
361 the decomposition structure of the 4-dimensional copula. As shown in the first row of Table 5, there is a

negative correlation between AMDF and RI for each station. The values of the Pearson correlation coefficients between AMDF and RI for AK, HJG and HZ stations are -0.37, -0.55 and -0.53, respectively, demonstrating that there is a significant relation between the reservoirs storage capacity and the reduction of AMDF. For each station, except for RRCI of one-dimensional case, the values of the Pearson, Kendall, and Spearman correlation coefficients between RRCI and AMDF are higher than between RI and AMDF. According to the highest Kendall correlation, the scheduling-related variables for the AK station are *M, I, V and T*; those for the HJG station are *I and T*; and those for the HZ station are *I, V and T*.

<Table 5>

Table 6 is the results of copula modeling of the scheduling-related variables, by aid of the R package “VineCopula” (<https://CRAN.R-project.org/package=VineCopula>). Note that for each bivariate pair in the third column of Table 6, three one-parameter bivariate Archimedean copula families (i.e., the Gumbel, Frank, and Clayton copulas) (Nelsen, 2006), are used to select from. As shown in Table 6, the results of the Cramer-von Mises test (Genest et al., 2009) show that all the C-vine copula models pass the test at the significant level of 0.05, indicating these models are effective for simulating the joint distribution of the scheduling-related variables for three stations. Finally, the variation of RI and RRCI over time is displayed in Figure 6. It is found that for each station, after reservoir construction, in most

379 cases, the annual values of RRCI are larger (close to 1) than those of RI. On the other hand, in few cases,
380 e.g., in 1983 at HZ and HJG stations, the RRCI values are lower than the RI values.

381 <Figure 6>

382 <Table 6>

383 4.3 Flood frequency analysis

384 In this section, nonstationary flood frequency analysis using RRCI or RI as covariate is
385 performed to investigate how reservoirs affect the downstream flood frequency. The summary of results
386 of fitting the nonstationary models to the flood data is shown in Table 7. Based on SBC, the lowest
387 values indicate that the best models for AK, HJG and HZ stations are the nonstationary WEI
388 distribution with S23, the nonstationary GA distribution with S21, and the nonstationary WEI
389 distribution with S21, hereafter referred to as WEI_S23, GA_S21, WEI_S21, respectively. Note that for
390 any one of the five distributions (i.e., GA, WEI, LOGNO, GU and GEV), the RRCI-dependent scenario
391 has a lower SBC value than the RI-dependent scenario for each gauging station. Furthermore, for the
392 RI-dependent and RRCI-dependent scenarios, taking the HZ station as an example, the optimal
393 formulas of two distribution parameters μ_t and σ_t are given as follows:

394 (1) WEI_S11

$$\begin{aligned}\mu_t &= \exp(9.94 - 2.79\text{RI}) \\ \sigma_t &= \exp(0.49)\end{aligned}\tag{13}$$

395

396 (2) WEI_S21

$$\begin{aligned}\mu_t &= \exp(9.92 - 1.42\text{RRCI}) \\ \sigma_t &= \exp(0.73)\end{aligned}\tag{14}$$

398 It is found that in the Eq. (13) and Eq. (14), there are the negative estimates of -2.79 and -1.42 for α_1 ,
399 respectively, revealing the decreasing degree of the frequency and magnitude of downstream floods due
400 to the reservoir effects.

401 Figure 7 compares the stationary scenario (S0), the RI-dependent scenario (S1), and the RRCI-
402 dependent scenario (S2) of the same optimal distributions in explaining all the flood values and the
403 several largest flood values for each station. The QQ plots (Figure 7a1, b1 and c1) show that overall, the
404 RRCI-dependent scenario captures more adequately the whole empirical quantiles (particularly the
405 smallest and largest empirical quantiles) than two other scenarios for each station. Furthermore, as
406 shown in Figure 7a2, b2 and c2, for the seven largest floods (observed) of each station, the RRCI-
407 dependent scenario produces lower quantile residuals than two other scenarios.

408 <Table 7>

409 <Figure 7>

410 Figure 8 presents the performance of the best models, i.e., WEI_S23 for AK station, GA_S21
411 for HJG station and WEI_S21 for HZ station. The points in the worm plots of Figure 8 are within the 95%
412 confidence intervals indicating that the selected models are reasonable. And according to the centile

curves plots of Figure 8, the AMFD series is well fitted by the best models. Undoubtedly, with the incorporation of the effects of MARI, the RRCI-dependent scenario well captures the presence of nonstationarity in the downstream flood frequency. Take the case of HZ station (Figure 8c1). After the construction of Danjiangkou Reservoir (1967), due to reservoir operation, most values of AMDF had been reduced in magnitude by this reservoir. However, some relatively large flood events still occurred several times, e.g., 25600 m³/s in 1983 and 19900 m³/s in 1975. Obviously, this phenomenon of flood occurrences is well explained by RRCI.

<Figure 8>

The 100-year return levels with the 95% credible interval from WEI_S23 and WEI_S13 for AK station, GA_S21 and GA_S11 for HJG station, and WEI_S21 and WEI_S11 for HZ station are presented in Figure 9. For each station, compared to the optimal RI-dependent distribution, the optimal RRCI-dependent distribution provides a lower 100-year return level but there exist exceptions, and provides a smaller uncertainty range. Besides, after the construction of the main reservoir, the uncertainty range of AK station is larger than HJG and HZ stations. The possible explanation to the larger uncertainty range is that the sample size (1993-2015) of the regulated floods at AK station is smaller, and, furthermore, the dependent relationship between RRCI and AMDF at AK station is weaker.

<Figure 9>

431 4.4 Discussion

432 The long-term variation of the AMDF series (Figure 8) indicates that the upstream reservoirs
433 have evidently altered the downstream flood regimes. As an example, since the completion of
434 Danjiangkou reservoir in 1967, the flood magnitude of HZ station is evidently reduced overall. This is
435 consistent with the results on the effects of reservoirs on the hydrological regime of this area in previous
436 literature (Cong et al., 2013; GUO et al., 2008; Jiang et al., 2014; Lu et al., 2009). In this study, it is
437 found that there is a significant difference between those downstream floods affected by the same
438 reservoir system (with the same RI value). In most cases, relative small downstream floods were
439 obtained. However, it is of interest to note that there still occurred unexpected large downstream floods
440 in few cases, in spite of a large RI value. For example, most values of AMDF in HZ station are less
441 10000 m³/s since 1967, but the values of AMDF in 1983 and in 1975 are 25600 m³/s and 19900 m³/s,
442 respectively. It is highlighted that those unexpected large downstream floods are probably related to the
443 MARI effects on reservoir operation. The five largest (unexpected) floods since 1967 and the
444 corresponding values of the scheduling-related MARI variables in the HZ station are shown in Table 8.
445 It is found that the largest floods of 1967-2015 occurred in 1983. For this flood event, the MARI is a
446 rare event (with the OR-JEP value of 0.435 ranking the second in 1967-2015) due to the largest mean
447 intensity ($I = 20.2$ mm) and the second late occurrence ($T = 281$). Surprisingly, all the timing values of
448 the MARI for these five unexpected downstream floods show the high rankings (2-9th). Those timing

449 values are near the end (about the 300th day of the year) of the flood control period (July-October) in
450 this area. Actually, near the end of the major flood control period, the storage capacity able to use
451 should be decreased, because according to the operation rules of Danjiangkou reservoir (Zhang et al.,
452 2009), there is a staged increasing flood limit water level in the flood control season. One important
453 cause for those unexpected large downstream floods is probably that the remaining storage capacity at
454 the end of flood season is not sufficient to reduce some late floods. Therefore, in addition to the own
455 storage capacity of reservoirs, the MARI effects should be indispensably considered when attempting to
456 accurately quantify the reservoir effects on downstream floods.

457 <Table 8>

458 With the combination of both RI and OR-JEP, RRCI has a significant difference from RI
459 (Figure 6). With a few exceptions, RRCI values are higher than RI values. It is indicated that the real
460 reservoir impact may be underestimated by RI in most cases. Moreover, RI will also probably
461 overestimate the real reservoir impact in few cases, because of no considering some special rainfall
462 events (i.e., the MARI with low values of OR-JEP). The results of the covariate-based nonstationary
463 flood frequency analysis (Table 7, Figure 7 and Figure 8) demonstrate that compared to the RI-
464 dependent scenario, the RRCI-dependent scenario for the optimal nonstationary distribution more
465 completely captures the presence of nonstationarity in the downstream flood frequency. Therefore,
466 RRCI might be a useful index in accessing the reservoir effects on the downstream flood frequency.

Finally, the estimation errors of OR-JEP should be noted. (1) Only those MARI samples which corresponds to the timing of AMDF are included to estimate OR-JEP; this means that some extreme MARI samples which corresponds to the non-maximum flow are not included, resulting in the estimation error for OR-JEP; to reduce this error, it might be worth considering the use of the peaks-over-threshold sampling method. (2) The areal-averaged MARI is based on the records of 16 rainfall stations with the IDW method; the estimation error of areal-averaged rainfall may be transferred to the OR-JEP estimation error; the additional rainfall site data and spatial distribution information are needed to reduce the OR-JEP estimation error. Nonetheless, the good performance of downstream flood frequency modeling demonstrates the MARI samples still remain representative in this study.

5 Conclusions

Accurately assessing the impact of reservoirs on downstream floods is an important issue for flood risk management. In this study, to evaluate the effects of reservoirs on downstream flood frequency of Hanjiang River, the rainfall-reservoir composite index (RRCI) is derived from the Eq. (2) which takes account of the combination of the reservoir index (RI) and the OR-joint exceedance probability (OR-JEP) of scheduling-related rainfall variables. The main findings are summarized as follows: (1) the magnitude of the downstream flood events has been reduced by the reservoir system in the study area; however, the long-term variation of the observed AMDF series show that despite of the large reservoirs, the unexpected large flood events still occurred several times, e.g., at Huangzhuang

station in 1983; and one important cause for the unexpected large floods of Huangzhuang station may be related to the operation strategy of staged increasing flood limit water level for Danjiangkou reservoir. (2) According to the results of the covariate-based nonstationary flood frequency analysis for each station, compared to the optimal RI-dependent distribution, the optimal RRCI-dependent distribution more completely captures the presence of nonstationarity in the downstream flood frequency. (3) Furthermore, in estimating 100-year return level for each station, the optimal RRCI-dependent distribution provides a lower 100-year return level but there exist exceptions, and provides a smaller uncertainty range associated with the uncertainty of model parameter.

Consequently, this study demonstrates the necessity of including the antecedent rainfall effects, in addition to the effects of reservoir storage capacity, on reservoir operation in assessing the reservoir effects on downstream flood frequency. The study might provide a comprehensive approach for the downstream flood risk management under the impacts of reservoirs.

Acknowledgments

This research is financially supported jointly by the National Natural Science Foundation of China (NSFC Grants 41890822 and 51525902), the Research Council of Norway (FRINATEK Project 274310), and the Ministry of Education “111 Project” Fund of China (B18037), all of which are greatly appreciated. We greatly appreciate the editor and the two reviewers for their insightful comments and

constructive suggestions for improving the manuscript. No conflict of interest exists in the submission of the manuscript.

References

Aas, K., Czado, C., Frigessi, A., Bakken, H., 2009. Pair-copula constructions of multiple dependence. Insurance: Mathematics and Economics, 44(2): 182-198. <https://doi.org/10.1016/j.insmatheco.2007.02.001>

Adlouni, S.E., Ouarda, T.B.M.J., Zhang, X., Roy, R., Bobée, B., 2007. Generalized maximum likelihood estimators for the nonstationary generalized extreme value model. Water Resources Research, 43(3): 455-456. <https://doi.org/10.1029/2005WR004545>.

Akaike, H., 1974. A new look at the statistical model identification. IEEE Transactions on Automatic Control, 19(6): 716-723. <https://doi.org/10.1109/TAC.1974.1100705>.

Ayalew, T.B., Krajewski, W.F., Mantilla, R., 2013. Exploring the effect of reservoir storage on peak discharge frequency. Journal of Hydrologic Engineering, 18(12): 1697-1708. [https://doi.org/10.1061/\(ASCE\)HE.1943-5584.0000721](https://doi.org/10.1061/(ASCE)HE.1943-5584.0000721).

Ayalew, T.B., Krajewski W.F., Mantilla R., 2015. Insights into Expected Changes in Regulated Flood Frequencies due to the Spatial Configuration of Flood Retention Ponds. Journal of Hydrologic Engineering, 20(10): [https://doi.org/10.1061/\(ASCE\)HE.1943-5584.0001173](https://doi.org/10.1061/(ASCE)HE.1943-5584.0001173)

Batalla, R.J., Gomez, C.M., Kondolf, G.M., 2004. Reservoir-induced hydrological changes in the Ebro River basin (NE Spain). Journal of Hydrology, 290(1-2): 117-136. <https://doi.org/10.1016/j.jhydrol.2003.12.002>

Benito, G., Thorndycraft, V.R., 2005. Palaeoflood hydrology and its role in applied hydrological sciences. Journal of Hydrology, 313(1-2): 3-15. <https://doi.org/10.1016/j.jhydrol.2005.02.002>.

Chib, S., Greenberg, E., 1995. Understanding the metropolis-hastings algorithm. The American Statistician, 49(4): 327-335. <https://doi.org/10.1080/00031305.1995.10476177>.

Chivers, C., 2012. MHadaptive: General Markov Chain Monte Carlo for Bayesian Inference using adaptive Metropolis-Hastings sampling. <https://CRAN.R-project.org/package=MHadaptive>

Coles, S., 2001. An introduction to statistical modeling of extreme values. <https://doi.org/10.1007/978-1-4471-3675-0>

531 Cong, M., Chunxia, L., Yiqiu, L., 2013. Runoff change in the lower reaches of Ankang Reservoir
532 and the influence of Ankang Reservoir on its downstream. *Resources and Environment in the Yangtze*
533 *Basin*, 22(11): 1433-1440.

534 Du, T. et al., 2015. Return period and risk analysis of nonstationary low-flow series under climate
535 change. *Journal of Hydrology*, 527: 234-250. <https://doi.org/10.1016/j.jhydrol.2015.04.041>

536 Genest, C., R émillard, B., Beaudoin, D., 2009. Goodness-of-fit tests for copulas: A review and a
537 power study. *Insurance: Mathematics and Economics*, 44(2): 199-213.
538 <https://doi.org/10.1016/j.insmatheco.2007.10.005>

539 Gilroy, K.L., Mccuen, R.H., 2012. A nonstationary flood frequency analysis method to adjust for
540 future climate change and urbanization. *Journal of Hydrology*, s 414–415(2): 40-48.
541 <https://doi.org/10.1016/j.jhydrol.2011.10.009>

542 Graf, W.L., 1999. Dam nation: A geographic census of American dams and their large - scale
543 hydrologic impacts. *Water resources research*, 35(4): 1305-1311.
544 <https://doi.org/10.1029/1999WR900016>

545 Goel, N.K., Kurothe, R.S., Mathur, B.S., Vogel, R.M., 1997. A derived flood frequency
546 distribution for correlated rainfall intensity and duration. *Water Resources Research*, 33(9): 2103–2107.
547 <https://doi.org/10.1029/97WR00812>

548 GUO, W.-x., XIA, Z.-q., WANG, Q., 2008. Effects of Danjiangkou Reservoir on hydrological
549 regimes in the middle and lower reaches of Hanjiang River. *Journal of Hohai University (Natural*
550 *Sciences)*, 36(6): 733-737. <https://doi.org/10.3876/j.issn.1000-1980.2008.06.002>

551 Jiang, C., Xiong, L., Xu, C.Y., Guo, S., 2014. Bivariate frequency analysis of nonstationary low-
552 flow series based on the time-varying copula. *Hydrological Processes*, 29(6): 1521-1534.
553 <https://doi.org/10.1002/hyp.10288>

554 Kwon, H.-H., Brown, C., Lall, U., 2008. Climate informed flood frequency analysis and
555 prediction in Montana using hierarchical Bayesian modeling. *Geophysical Research Letters*, 35(5).
556 <https://doi.org/10.1029/2007GL032220>

557 L ópez, J., Franc és, F., 2013. Non-stationary flood frequency analysis in continental Spanish rivers,
558 using climate and reservoir indices as external covariates. *Hydrology and Earth System Sciences*, 17(8):
559 3189-3203. <https://doi.org/10.5194/hess-17-3189-2013>

560 Lee, J., Heo, J.-H., Lee, J., Kim, N., 2017. Assessment of Flood Frequency Alteration by Dam
561 Construction via SWAT Simulation. *Water*, 9(4): 264. <https://doi.org/10.3390/w9040264>

562 Liang, Z. et al., 2017. A sample reconstruction method based on a modified reservoir index for
563 flood frequency analysis of non-stationary hydrological series. Stochastic Environmental Research and
564 Risk Assessment: 1-11. <https://doi.org/10.1007/s00477-017-1465-1>

565 Lu, G.-b., Liu, Y., Zou, X.-l., Zou, Z.-h., Cai, T., 2009. Impact of the Danjiangkou Reservoir on
566 the flow regime in the middle and lower reaches of Hanjiang River. Resources and Environment in the
567 Yangtze Basin, 18(10): 959-963.

568 Magilligan, F.J., Nislow, K.H., 2005. Changes in hydrologic regime by dams. Geomorphology,
569 71(1-2): 61-78. <https://doi.org/10.1016/j.geomorph.2004.08.017>

570 Martins, E.S., Stedinger, J.R., 2000. Generalized maximum-likelihood generalized extreme-value
571 quantile estimators for hydrologic data. Water Resources Research, 36(3): 737-744.
572 <https://doi.org/10.1029/1999WR900330>

573 Martins, E.S., Stedinger, J.R., 2001. Generalized maximum likelihood Pareto-Poisson estimators
574 for partial duration series. Water Resources Research, 37(10): 2551-2557.

575 Mei, X., Dai, Z., Van Gelder, P.H.A.J.M., and Gao, J., 2015. Linking Three Gorges Dam and
576 downstream hydrological regimes along the Yangtze River, China. Earth and Space Science, 2(4): 94-
577 106. <https://doi.org/10.1002/2014EA000052>

578 Milly, P.C.D. et al., 2008. Stationarity Is Dead: Whither Water Management? Science, 319(5863):
579 573-4. <https://doi.org/10.1029/2001WR000367>

580 Nelsen, R., 2006. An Introduction to Copulas . NY: Springer Science+ Business Media. Inc.
581 <https://doi.org/10.1007/0-387-28678-0>

582 Ouarda, T., and S. El - Adlouni (2011), Bayesian nonstationary frequency analysis of
583 hydrological variables 1, JAWRA Journal of the American Water Resources Association, 47(3), 496-
584 505. <https://doi.org/10.1111/j.1752-1688.2011.00544.x>

585 Pettitt, A.N., 1979. A Non-Parametric Approach to the Change-Point Problem. Journal of the
586 Royal Statistical Society, 28(2): 126. <https://www.jstor.org/stable/2346729>

587 Reis Jr, D.S., Stedinger, J.R., 2005. Bayesian MCMC flood frequency analysis with historical
588 information. Journal of hydrology, 313(1-2): 97-116. <https://doi.org/10.1016/j.jhydrol.2005.02.028>

589 Ribatet, M., Sauquet, E., Gréillon, J.-M., Ouarda, T.B., 2007. Usefulness of the reversible jump
590 Markov chain Monte Carlo model in regional flood frequency analysis. Water Resources Research,
591 43(8). <https://doi.org/10.1029/2006WR005525>

592 Rigby, R.A., Stasinopoulos, D.M., 2005. Generalized additive models for location, scale and
593 shape. *Appl. Statist.*, 54(3): 507-554. <https://doi.org/10.1111/j.1467-9876.2005.00510.x>

594 Salas, J.D. (1993) Analysis and Modeling of Hydrologic Time Series. In: Maidment, D.R., Ed.,
595 Handbook of Hydrology, McGraw-Hill, New York, 19.1-19.72.

596 Scarf, P., 1992. Estimation for a four parameter generalized extreme value distribution.
597 *Communications in Statistics-Theory and Methods*, 21(8): 2185-2201.
598 <https://doi.org/10.1080/03610929208830906>

599 Schwarz, G., 1978. Estimating the dimension of a model. *The Annals of Statistics*, 6(2), 461-464.

600 Sklar, M., 1959. Fonctions de repartition an dimensions et leurs marges. *Publications de l'Institut*
601 *Statistique de l'Université de Paris*, 8: 229-231.

602 Su, C., Chen, X., 2018. Assessing the effects of reservoirs on extreme flows using nonstationary
603 flood frequency models with the modified reservoir index as a covariate. *Advances in Water Resources*.
604 <https://doi.org/10.1016/j.advwatres.2018.12.004>

605 Viglione, A., Merz, R., Salinas, J.L., Blöschl, G., 2013. Flood frequency hydrology: 3. A
606 Bayesian analysis. *Water Resources Research*, 49(2): 675-692. <https://doi.org/10.1029/2011WR010782>

607 Villarini, G. et al., 2009. Flood frequency analysis for nonstationary annual peak records in an
608 urban drainage basin. *Advances in Water Resources*, 32(8): 1255-1266.
609 <https://doi.org/10.1016/j.advwatres.2009.05.003>

610 Volpi, E., Di Lazzaro M., Bertola M., Viglione A., and Fiori A., 2018. Reservoir Effects on Flood
611 Peak Discharge at the Catchment Scale. *Water Resources Research*, 54(11): 9623-9636.
612 <https://doi.org/10.1029/2018WR023866>

613 Wang, W. et al., 2017. Nonlinear filtering effects of reservoirs on flood frequency curves at the
614 regional scale. *Water Resources Research*, 53(10): 8277-8292. <https://doi.org/10.1002/2017WR020871>

615 Wyżga, B., Kundzewicz, Z.W., Ruiz-Villanueva, V., Zawiejska, J., 2016. Flood generation
616 mechanisms and changes in principal drivers, Flood Risk in the Upper Vistula Basin. Springer, pp. 55-
617 75. https://doi.org/10.1007/978-3-319-41923-7_4

618 Xiong, B., Xiong, L., Chen, J., Chong-Yu, X., Li, L., 2018. Multiple causes of nonstationarity in
619 the Weihe annual low-flow series. *Hydrology and Earth System Sciences*, 22(2): 1525.
620 <https://doi.org/10.5194/hess-22-1525-2018>

621 Xiong, L., Jiang, C., Xu, C.Y., Yu, K.X., Guo, S., 2015. A framework of change-point detection
622 for multivariate hydrological series. *Water Resources Research*, 51(10): 8198-8217.
623 <https://doi.org/10.1002/2015WR017677>

624 Yan, L., Xiong, L., Liu, D., Hu, T., Xu, C.Y., 2017. Frequency analysis of nonstationary annual
625 maximum flood series using the time-varying two-component mixture distributions. *Hydrological*
626 *Processes*, 31(1): 69-89. <https://doi.org/10.1002/hyp.10965>

627 Yang, T., Zhang Q., Chen Y.D., Tao X., Xu C.Y., and Chen X., 2008. A spatial assessment of
628 hydrologic alteration caused by dam construction in the middle and lower Yellow River, China.
629 *Hydrological Processes: An International Journal*, 22(18): 3829-3843. <https://doi.org/10.1002/hyp.6993>

630 Zhang L., Xu J., Huo, J., Chen J., 2009. Study on Stage Flood Control Water Level of
631 Danjiangkou Reservoir. *Journal of Yangtze River Scientific Research Institute*, 26 (3): 13-14. (In
632 Chinese)

633 Zhang, Q., Gu, X., Singh, V.P., Xiao, M., Chen, X., 2015. Evaluation of flood frequency under
634 non-stationarity resulting from climate indices and reservoir indices in the East River basin, China.
635 *Journal of Hydrology*, 527: 565-575. <https://doi.org/10.1016/j.jhydrol.2015.05.029>

636

637 **Tables**

638 **Table 1. Summary of the probability density functions, the corresponding moments and the used**
639 **link functions for nonstationary flood frequency analysis.**

Distributions	Probability density functions	Moments	Link functions
Gamma (GA)	$f_Y(y \mu_i, \sigma_i) = \frac{(y)^{1/\sigma_i^2-1}}{\Gamma(1/\sigma_i^2)(\mu\sigma_i^2)^{1/\sigma_i^2}} \exp\left(-\frac{y}{\mu_i\sigma_i^2}\right)$ $y > 0, \mu_i > 0, \sigma_i > 0$	$E(Y) = \mu_i$ $Var(Y) = \mu_i^2 \sigma_i^2$	$g_1(\mu_i) = \ln(\mu_i)$ $g_2(\sigma_i) = \ln(\sigma_i)$
Weibull (WEI)	$f_Y(y \mu_i, \sigma_i) = \left(\frac{\sigma_i}{\mu_i}\right) \left(\frac{y}{\mu_i}\right)^{\sigma_i-1} \exp\left(-\left(\frac{y}{\mu_i}\right)^{\sigma_i}\right)$ $y > 0, \mu_i > 0, \sigma_i > 0$	$E(Y) = \mu_i \Gamma(1+1/\sigma_i)$ $Var(Y) = \mu_i^2 [\Gamma(1+2/\sigma_i) - \Gamma^2(1+1/\sigma_i)]$	$g_1(\mu_i) = \ln(\mu_i)$ $g_2(\sigma_i) = \ln(\sigma_i)$
Lognormal (LOGNO)	$f_Y(y \mu_i, \sigma_i) = \frac{1}{y\sigma_i\sqrt{2\pi}} \exp\left\{-\frac{[\log(y)-\mu_i]^2}{2\sigma_i^2}\right\}$ $y > 0, -\infty < \mu_i < \infty, \sigma_i > 0$	$E(Y) = w^{1/2} \exp(\mu_i)$ $Var(Y) = w(w-1) \exp(2\mu_i)$ $w = \exp(\sigma_i^2)$	$g_1(\mu_i) = \ln(\mu_i)$ $g_2(\sigma_i) = \ln(\sigma_i)$
Gumbel (GU)	$f_Y(y \mu_i, \sigma_i) = \frac{1}{\sigma_i} \exp\left\{\left[\left(\frac{y-\mu_i}{\sigma_i}\right) - \exp\left(\frac{y-\mu_i}{\sigma_i}\right)\right]\right\}$ $-\infty < y < \infty, -\infty < \mu_i < \infty, \sigma_i > 0$	$E(Y) = \mu_i - 0.57722\sigma_i$ $Var(Y) = (\pi^2/6)\sigma_i^2$	$g_1(\mu_i) = \mu_i$ $g_2(\sigma_i) = \ln(\sigma_i)$
Generalized Extreme Value (GEV)	$f_Y(y \mu_i, \sigma_i, \xi) = \frac{1}{\sigma_i} \left[1 + \xi\left(\frac{y-\mu_i}{\sigma_i}\right)\right]^{-1/\xi-1} \exp\left\{-\left[1 + \xi\left(\frac{y-\mu_i}{\sigma_i}\right)\right]^{-1/\xi}\right\}$ $y > \mu_i - \sigma_i/\xi, -\infty < \mu_i < \infty, \sigma_i > 0, -\infty < \xi < \infty$	$E(Y) = \mu_i - \frac{\sigma_i}{\xi} + \frac{\sigma_i}{\xi} \eta_1$ $Var(Y) = \sigma_i^2 (\eta_2 - \eta_1^2) / \xi$ $\eta_m = \Gamma(1 - m\xi)$	$g_1(\mu_i) = \mu_i$ $g_2(\sigma_i) = \ln(\sigma_i)$

640

641

642

Table 2. Seven nonstationary scenarios for the formulas of the two distribution parameters (i.e., μ_t and σ_t).

Scenario classification	Scenario codes	The formula of distribution parameters	
		$g_1(\mu_t)$	$g_2(\sigma_t)$
Stationary (S0)	S0	α_0	β_0
RI-dependent (S1)	S11	$\alpha_0 + \alpha_1 \text{RI}$	β_0
	S12	α_0	$\beta_0 + \beta_1 \text{RI}$
	S13	$\alpha_0 + \alpha_1 \text{RI}$	$\beta_0 + \beta_1 \text{RI}$
RRCI-dependent (S2)	S21	$\alpha_0 + \alpha_1 \text{RRCI}$	β_0
	S22	α_0	$\beta_0 + \beta_1 \text{RRCI}$
	S23	$\alpha_0 + \alpha_1 \text{RRCI}$	$\beta_0 + \beta_1 \text{RRCI}$

648

Table 3. Information of the five major reservoirs in Hanjiang River basin.

Reservoirs	Longitude	Latitude	Area (km ²)	Year	Capacity (10 ⁹ m ³)
Shiquan	108.05	33.04	23400	1974	0.566
Ankang	108.83	32.54	35700	1992	3.21
Huanglongtan	110.53	32.68	10688	1978	1.17
Dangjiangkou	111.51	32.54	95220	1967	34.0
Yahekou	112.49	33.38	3030	1960	1.32

649

650

651

Table 4. Change in the mean and standard deviation of AMDF after the construction of the two large reservoirs (i.e., Danjiangkou reservoir completed by 1967, and Ankang reservoir built by 1992).

Stations	Mean (m ³ /s)			Standard deviation (m ³ /s)		
	1956-1966	1967-1991	1992-2015	1956-1966	1967-1991	1992-2015
AK	9451	10468	6506	4341	4623	4454
HJG	14951	7524	4139	7896	5482	4074
HZ	16603	10120	5958	8833	5420	4721

661

Table 5. Correlation coefficients between RRCI and AMDF.

Subset of rainfall variables	AK			HJG			HZ		
	Pearson	Kendall	Spearman	Pearson	Kendall	Spearman	Pearson	Kendall	Spearman
-*	-0.37	-0.18	-0.28	-0.55	-0.37	-0.54	-0.53	-0.38	-0.55
<i>M</i>	-0.27	-0.27	-0.37	-0.67	-0.53	-0.74	-0.45	-0.37	-0.51
<i>I</i>	-0.26	-0.25	-0.34	-0.74	-0.57	-0.79	-0.54	-0.41	-0.56
<i>V</i>	-0.32	-0.28	-0.39	-0.63	-0.49	-0.69	-0.57	-0.48	-0.65
<i>T</i>	-0.11	-0.17	-0.24	-0.68	-0.55	-0.73	-0.48	-0.40	-0.57
<i>M, I</i>	-0.37	-0.28	-0.38	-0.70	-0.56	-0.77	-0.56	-0.43	-0.58
<i>M, V</i>	-0.42	-0.29	-0.40	-0.64	-0.50	-0.71	-0.56	-0.45	-0.60
<i>M, T</i>	-0.37	-0.26	-0.36	-0.69	-0.57	-0.77	-0.64	-0.46	-0.63
<i>I, V</i>	-0.46	-0.31	-0.42	-0.71	-0.54	-0.76	-0.65	-0.50	-0.67
<i>I, T</i>	-0.34	-0.22	-0.31	-0.73	-0.60	-0.80	-0.68	-0.50	-0.66
<i>V, T</i>	-0.43	-0.28	-0.39	-0.68	-0.55	-0.75	-0.69	-0.52	-0.71
<i>M, I, V</i>	-0.49	-0.31	-0.42	-0.65	-0.53	-0.74	-0.63	-0.47	-0.63
<i>M, I, T</i>	-0.41	-0.27	-0.37	-0.68	-0.57	-0.78	-0.67	-0.49	-0.66
<i>M, V, T</i>	-0.50	-0.29	-0.40	-0.65	-0.56	-0.76	-0.67	-0.49	-0.67
<i>I, V, T</i>	-0.51	-0.31	-0.41	-0.67	-0.58	-0.78	-0.71	-0.53	-0.70
<i>M, I, V, T</i>	-0.53	-0.31	-0.42	-0.65	-0.57	-0.77	-0.69	-0.52	-0.69

*The values in the first row are the correlation coefficients between RI and flood series

662

663

664 Table 6. Results of copula models for scheduling-related rainfall variables.

Stations	Scheduling-related variables	Pairs	Copula type	Parameters θ_c	Kendall's tau	Goodness-of-fit test based on the empirical copula	
						CvM*	p-value
AK	M, I, V, T	14	Clayton	0.16	0.08	0.169	0.860
		13	Clayton	1.28	0.39		
		12	Clayton	1.01	0.33		
		24 1	Frank	1.21	0.17		
		23 1	Frank	-2.24	-0.24		
		34 12	Clayton	0.96	0.11		
HJG	I, T	24	Clayton	1.37	0.41	0.473	0.425
HZ	I, V, T	24	Gumbel	1.12	0.11	0.181	0.820
		23	Clayton	1.31	0.40		
		34 2	Clayton	0.49	0.20		

665 * CvM is the statistic of the Cramer-von Mises test; if the p-value of the C-vine copula model is less than the significance level of 0.05, the model is considered to be
666 not consistent with the empirical copula.

667

668

Table 7. Summary of results of the nonstationary flood distribution models.

Stations	Covariates	Distributions	The optimal formulas* of distribution parameters				AIC	SBC
			Selected models	μ_t	σ_t	ξ		
AK	RI	GA	WEI_S23	exp(9.24-2.64RI)	exp(-0.769+2.9RI)	-	1177.2	1185.5
	RI	WEI		exp(9.36-2.83RI)	exp(0.882-3.18RI)	-	1176.9	1185.3
	RI	LOGNO		exp(9.14-3.86RI)	exp(-0.716+3.28RI)	-	1180.4	1188.8
	RI	GU		11875-13093RI	exp(8.5)	-	1199.6	1205.9
	RI	GEV		7685-15252RI	exp(8.3)	-0.043	1182.3	1190.6
	RRCI	GA		exp(9.28-1.11RRCI)	exp(-0.825+0.689RRCI)	-	1165.3	1173.7
	RRCI	WEI		exp(9.4-1.17RRCI)	exp(0.982-0.884RRCI)	-	1163.8	1172.2
	RRCI	LOGNO		exp(9.19-1.33RRCI)	exp(-0.749+0.677RRCI)	-	1168.0	1176.4
	RRCI	GU		12555-7535RRCI	exp(8.4)	-	1188.0	1194.2
	RRCI	GEV		8460-6722RRCI	exp(8.2)	-0.096	1172.1	1180.5
HJG	RI	GA	GA_S21	exp(9.7-1.62RI)	exp(-0.25)	-	1139.9	1146.0
	RI	WEI		exp(9.75-1.56RI)	exp(0.27)	-	1141.4	1147.5
	RI	LOGNO		exp(9.47-1.8RI)	exp(-0.17)	-	1140.9	1147.1
	RI	GU		17955-14399RI	exp(8.8)	-	1189.5	1195.7
	RI	GEV		6976-5930RI	exp(8.79-1.49RI)	0.43	1149.9	1160.2
	RRCI	GA		exp(9.99-1.99RRCI)	exp(-0.45)	-	1112.5	1118.6
	RRCI	WEI		exp(10.1-1.97RRCI)	exp(0.53)	-	1113.2	1119.4
	RRCI	LOGNO		exp(9.75-1.94RRCI)	exp(-0.38)	-	1113.9	1120.1
	RRCI	GU		23067-20871RRCI	exp(9.2-1.7RRCI)	-	1121.3	1129.6
	RRCI	GEV		12113-10683RRCI	exp(9.2-2.01RRCI)	0.051	1112.5	1122.8
HZ	RI	GA	WEI_S21	exp(9.85-2.87RI)	exp(-0.42)	-	1198.3	1204.9
	RI	WEI		exp(9.94-2.79RI)	exp(0.49)	-	1198.6	1204.9
	RI	LOGNO		exp(9.63-2.93RI)	exp(-0.33)	-	1201.1	1207.4
	RI	GU		18661-23706RI	exp(8.8)	-	1237.5	1243.7
	RI	GEV		9605-13545RI	exp(9.03-2.56RI)	0.099	1207.8	1218.3
	RRCI	GA		exp(9.85-1.52RRCI)	exp(-0.61)	-	1173.1	1179.4
	RRCI	WEI		exp(9.92-1.42RRCI)	exp(0.73)	-	1171.2	1177.5
	RRCI	LOGNO		exp(9.72-1.55RRCI)	exp(-0.51)	-	1178.7	1185.0
	RRCI	GU		19214-14344RRCI	exp(8.86-0.881RRCI)	-	1189.7	1198.1
	RRCI	GEV		12502-9911RRCI	exp(8.96-1.37RRCI)	-0.068	1176.0	1186.4

*The model parameters in the optimal formulas are the posterior mean from Bayesian inference.

674 Table 8. Summary of the rainfall information for the five largest floods after the construction
675 (1967) of Danjiangkou reservoir in HZ station.

Year	Values (Ranking in 1967-2015)				
	AMDF [m ³ /s]	OR_JEP [-]	<i>I</i> [mm]	<i>V</i> [mm]	<i>T</i> [day of the year]
1983	25600 (1)	0.435 (2)	20.2 (1)	121.4 (19)	281 (2)
1975	19900 (2)	0.557 (7)	9.6 (18)	163.6 (13)	277 (6)
1974	18200 (3)	0.506 (4)	12.0 (7)	120.4 (20)	278 (4)
2005	16800 (4)	0.651 (11)	8.2 (27)	179.7 (10)	278 (4)
1984	16100 (5)	0.461 (3)	9.9 (15)	256.3 (4)	273 (9)

677

678

680

681

682

683

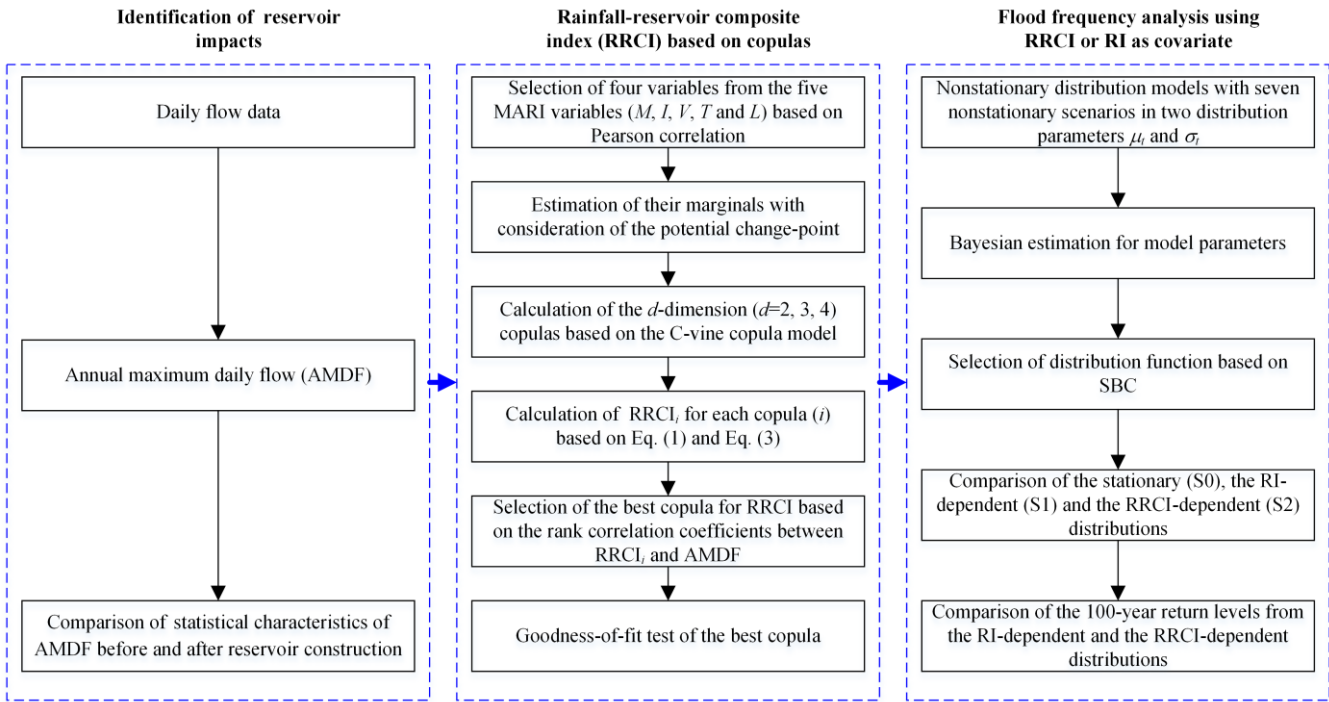


Figure 1. Flowchart of nonstationary covariate-based flood frequency analysis with a rainfall-reservoir composite index (RRCI).

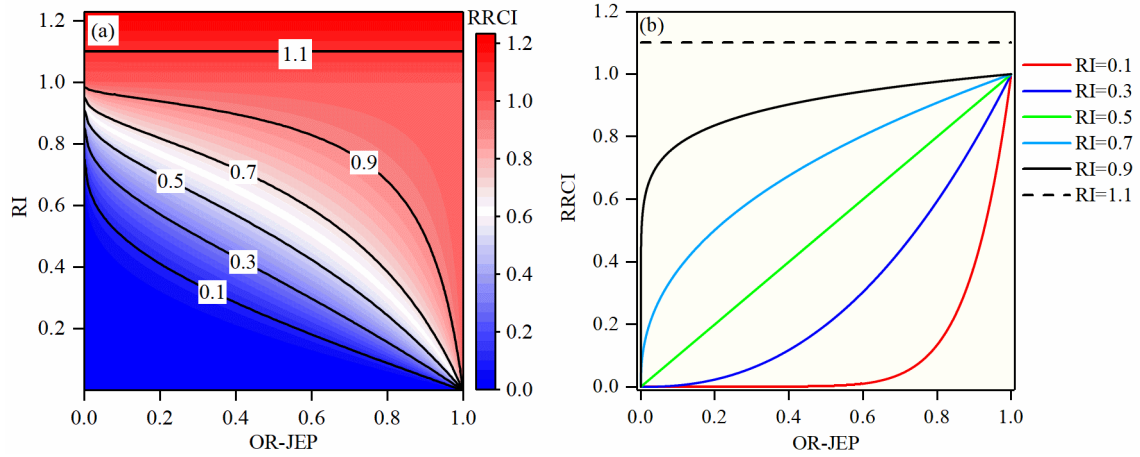
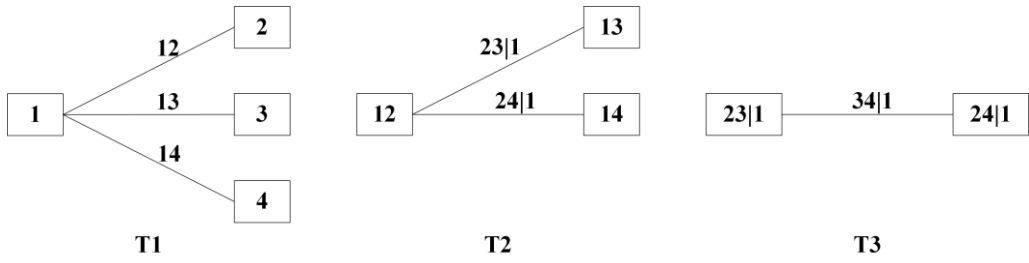


Figure 2. Relationship in the Eq. (2). (a) is the contour plot of RRCI against both RI and OR-JEP;

(b) is the function curves of RRCI against OR-JEP under the different values of RI.

688



689

Figure 3. Decomposition of a C-vine copula with four variables and 3 trees (denoted by T1, T2

690

and T3).

691

692

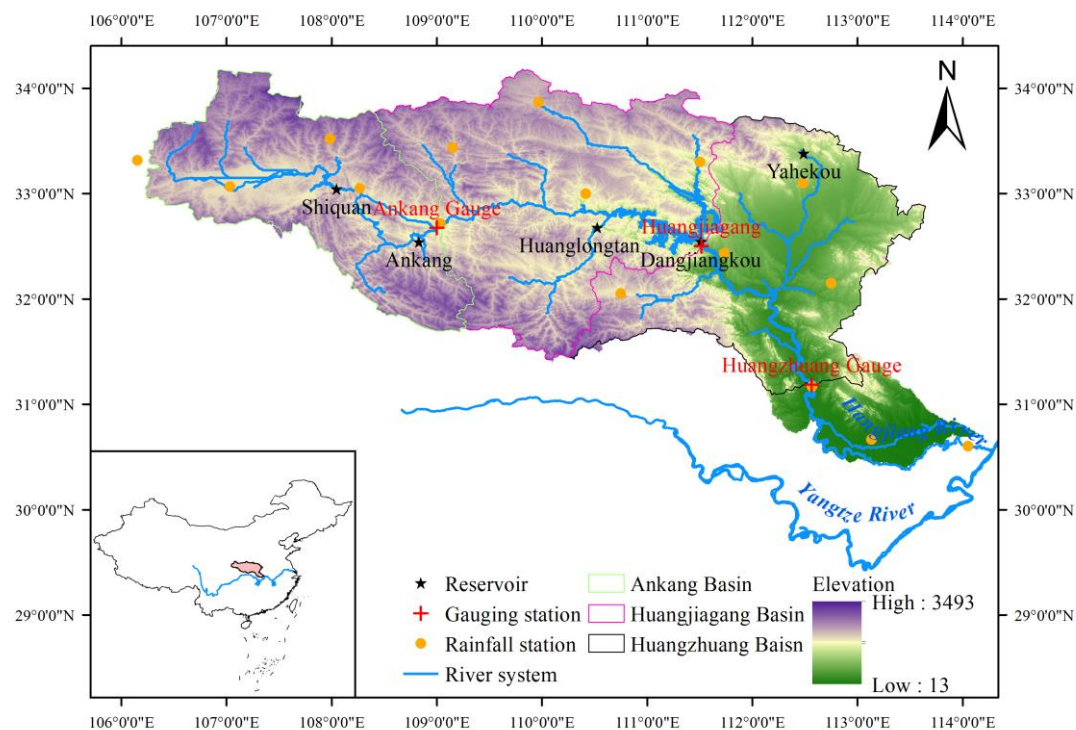


Figure 4. Geographic location of the reservoirs, gauging stations and rainfall stations in Hanjiang River.

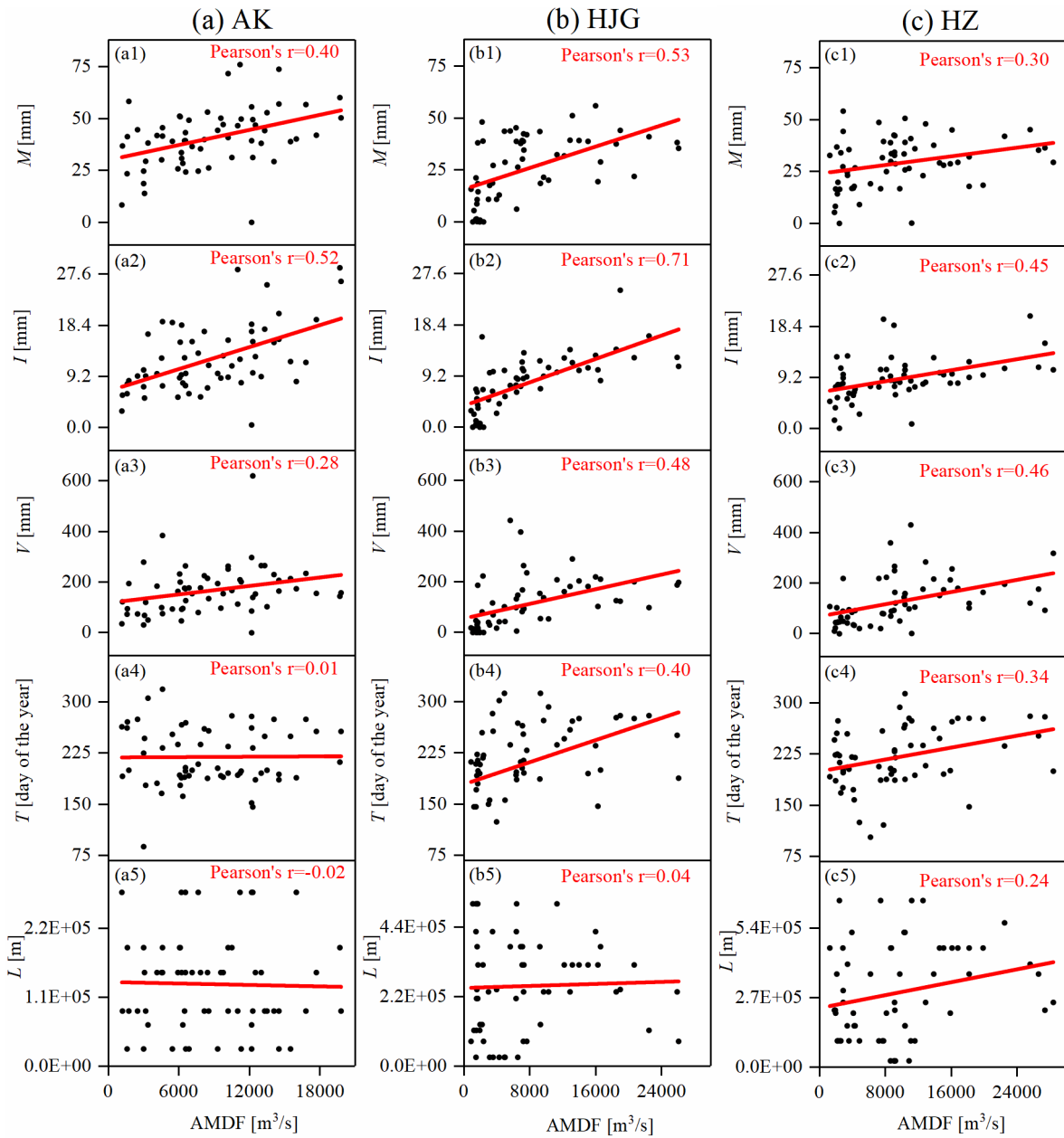


Figure 5. Linear correlation between the five MARI variables and AMDF for (a) AK station, (b) HJG station and (c) HZ station.

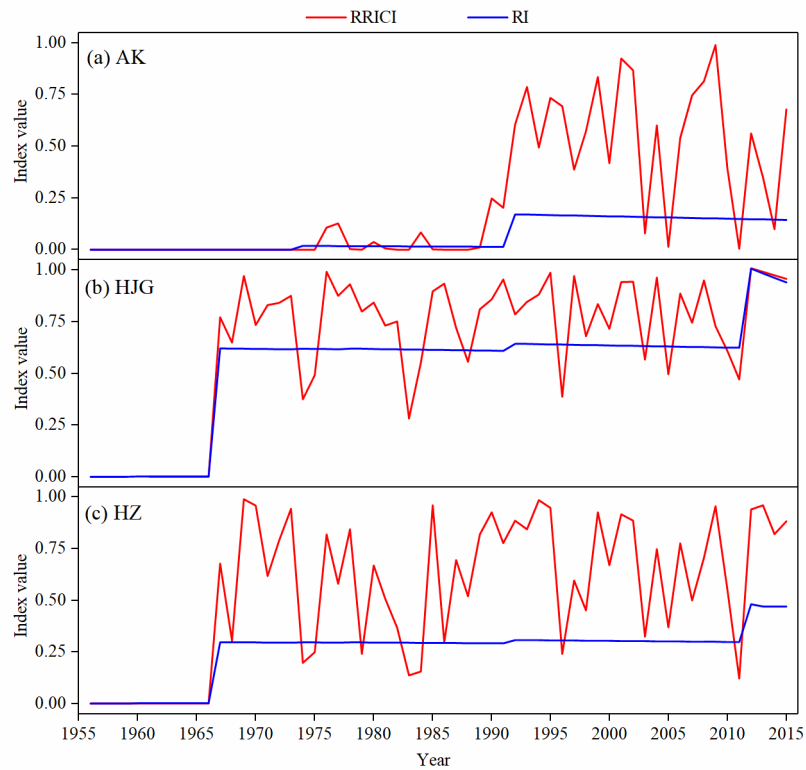


Figure 6. Variation of RI and RRICI for (a) AK station, (b) HJG station and (c) HZ station.

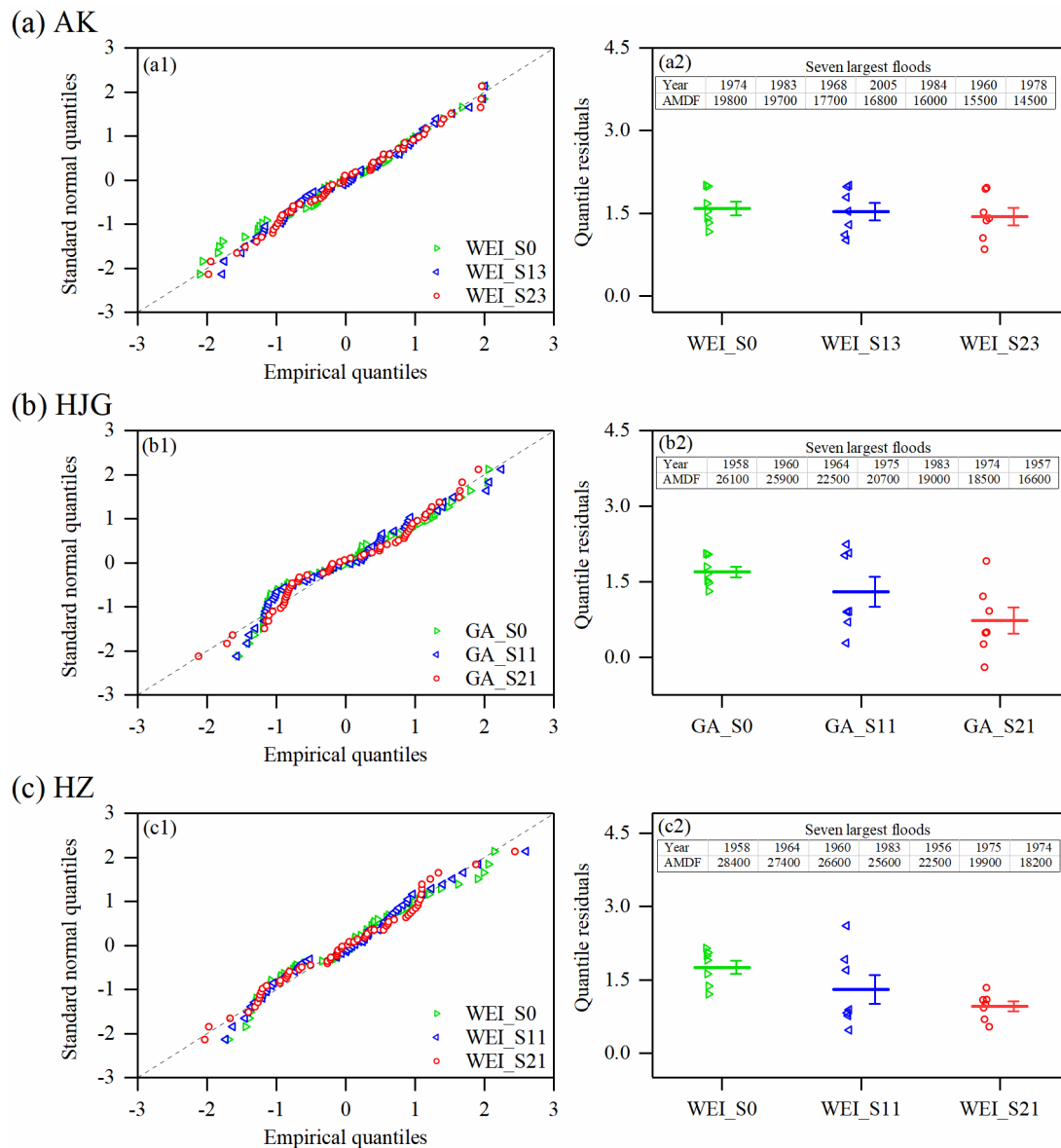


Figure 7. Comparison of the stationary (S0), the RI-dependent (S1) and the RRCI-dependent (S2) scenarios of the same optimal distributions for (a) AK station, (b) HJG station and (c) HZ station. The left panels (a1, b1 and c1) are the QQ plots for the whole AMDF series in each station. The right panels (a2, b2 and c2) are the plots of quantile residuals for the seven largest floods (their values and

711 occurrence years have been listed) in each station, and the means of their quantile residuals (points) and
712 the corresponding standard errors are indicated by the lines.

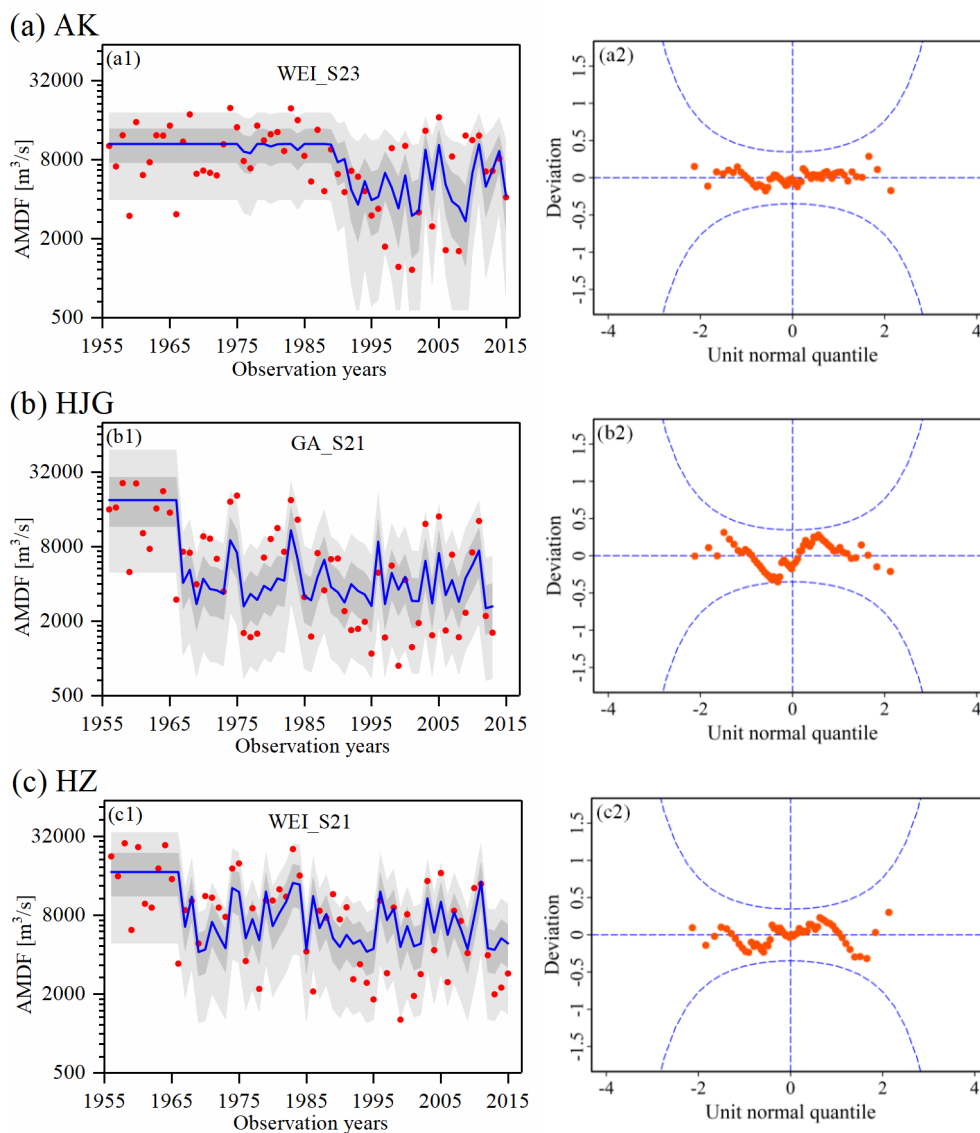


Figure 8. Performance of (a) WEI_S23 for AK station, (b) GA_S21 for HJG station and (c)

WEI_S21 for HZ station. The left panels (a1, b1 and c1) are the centile curves plots in each station (the 50th centile curves are indicated by the thick blue lines; the light gray-filled areas are between the 5th and 95th centile curves; the dark grey-filled areas are between the 25th and 75th centile curves; the

721 filled red points indicate the observed series). The right panels (a2, b2 and c2) are the worm plots; a
722 reasonable model should have the plotted points within the 95% confidence intervals (between the two
723 blue dashed curves).

724

725

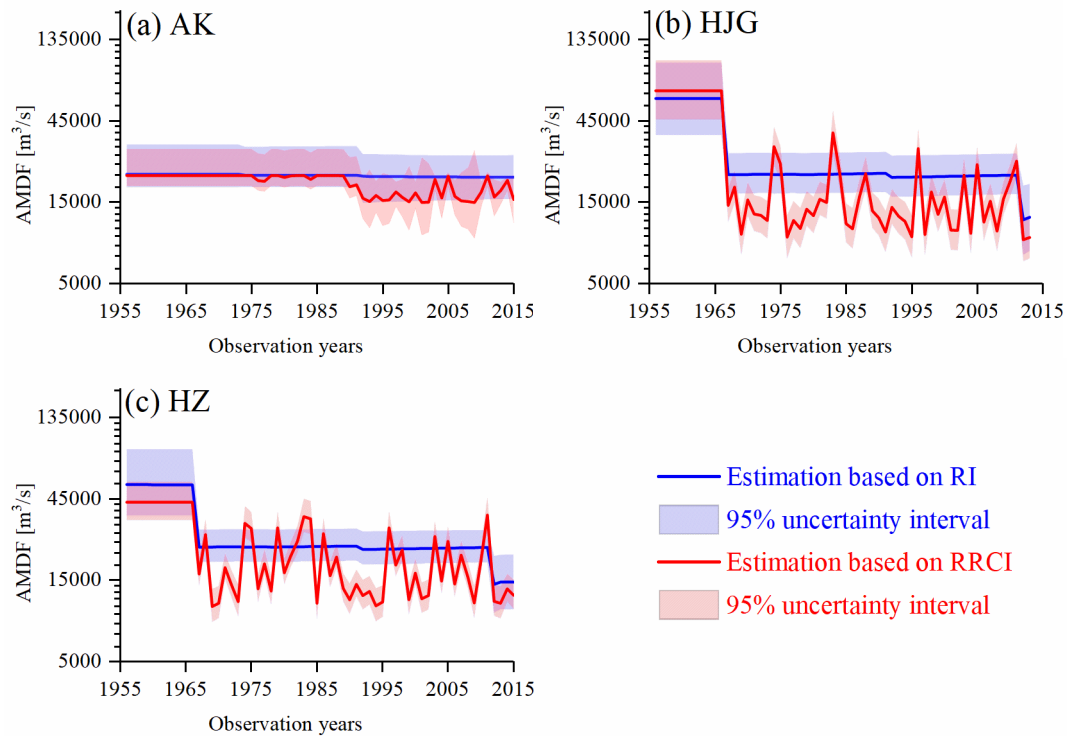


Figure 9. Statistical inference of the 100-year return levels with the 95% uncertainty interval using the optimal RI-dependent and RRCI-dependent distributions: (a) WEI_S13 and WEI_S23 for AK station, (b) GA_11 and GA_S21 for HJG station, and (c) WEI_S11 and WEI_S21 for HZ station.